

1                   **Counter-electrojet occurrence as observed from C/NOFS**  
2                   **satellite and ground-based magnetometer data over the African**  
3                   **and American sectors**

4                   **John Bosco Habarulema<sup>1,2</sup>, Gabrielle Lefebvre<sup>3</sup>, Mark B. Moldwin<sup>3</sup>, Zama T**  
5                   **Katamzi-Joseph<sup>1,2</sup>, and Endawoke Yizengaw<sup>4</sup>**

6                   <sup>1</sup>South African National Space Agency, P.O Box 32, Hermanus 7200, South Africa.

7                   <sup>2</sup>Department of Physics and Electronics, Rhodes University, South Africa.

8                   <sup>3</sup>Department of Climate and Space Sciences and Engineering, University of Michigan, Ann Arbor, Michigan, USA.

9                   <sup>4</sup>Space Science Application Laboratory, The Aerospace Corporation, El Segundo, CA, USA.

10                   **Key Points:**

- 11                   • A statistical trend of counter-electrojet (CEJ) events using C/NOFS satellite vertical  
12                   ion plasma drift and magnetometer observations has been established.
- 13                   • Both C/NOFS satellite and magnetometer data show higher CEJ occurrence rate  
14                   over the African sector than the American sector
- 15                   • C/NOFS satellite data exhibits more CEJ events than magnetometer data by average  
16                   of about 20% and 40% over the American and African sectors respectively.

This is the author manuscript accepted for publication and has undergone full peer review but has not been through the copyediting, typesetting, pagination and proofreading process, which may lead to differences between this version and the [Version of Record](#). Please cite this article as doi: [10.1029/2019SW002236](https://doi.org/10.1029/2019SW002236)

Corresponding author: John Bosco Habarulema, [jhabarulema@sansa.org.za](mailto:jhabarulema@sansa.org.za)

**Abstract**

An analysis of the counter-electrojet occurrence (CEJ) during 2008-2014 is presented for the African and American sectors based on local daytime (0700-1700 LT) observations from the Communications and Navigation Outage Forecasting System (C/NOFS) vertical ion plasma drift (equivalent to vertical  $\mathbf{E} \times \mathbf{B}$  at altitude of about 400 km) and ground-based magnetometers. Using quiet time ( $K_p \leq 3$ ) data, differences and/or similarities between the two datasets with reference to local time and seasonal dependence are established. For the first time, it is shown that C/NOFS satellite data are consistent with magnetometer observations in identifying CEJ occurrences during all seasons. However, C/NOFS satellite data show higher CEJ occurrence rate for almost all seasons. With respect to local time, C/NOFS satellite observes more CEJ events than magnetometer observations by average of about 20% and 40% over the American and African sectors respectively, despite both datasets showing similar trends in CEJ identification. Therefore, when a space weather event occurs, it is important to first establish the original variability nature and/or magnitude of the eastward electric field in equatorial regions before attributing the resulting changes to solar wind-magnetosphere and ionosphere coupling processes since CEJ events can be present even during quiet conditions.

**1 Introduction**

The equatorial electrojet (EEJ) is a natural phenomenon within the E-region ionosphere and is a result of electric fields driven from neutral wind dynamics and geomagnetic field geometry at the equator. EEJ is a strip of current that flows within about  $\pm 3^\circ$  latitudes from the geomagnetic equator and is usually eastward during daytime. Sometimes, the direction of the current reverses to westward, a phenomena called counter electrojet (CEJ) due to a number of physical mechanisms including (but not limited to), ionospheric variability during stratospheric warming periods [Stening *et al.*, 1996; Vineeth *et al.*, 2009; Siddiqui *et al.*, 2018], westward prompt penetrating electric field leading to ionospheric disturbed dynamo [Kikuchi *et al.*, 2000; Yizengaw *et al.*, 2011] and vertical upward winds uplifting ions thereby cancelling the vertical polarization electric field [Raghavarao and Anandarao, 1980]. Therefore the complex variability of CEJ is influenced/modulated by variations in local time, longitude (mainly related to migrating and non-migrating tides), seasonal dependence, lunar cycles, magnetic activity and solar activity [Rastogi, 1974; Mayaud, 1977; Marriott *et al.*, 1979; Rabiou *et al.*, 2017; Singh *et al.*, 2018; Soares *et al.*,

2018; Zhou et al., 2018]. Since the CEJ's first detection [Gouin, 1962], various studies have investigated the CEJ occurrence based mainly on magnetometers deployed in equatorial and/or low-latitude regions [e.g., Rastogi, 1974; Alex and Mukherjee, 2001, and references therein]. With time, the emergence of Low Earth Orbit (LEO) satellites in conducting ionosphere-thermosphere investigations such as Magnetic Field Satellite (MAGSAT), Republic of China Satellite, ROCSAT, Challenging Minisatellite Payload (CHAMP), Communications and Navigation Outage Forecasting System (C/NOFS), and SWARM, LEO measurements became complementary data sources for EEJ or CEJ studies [e.g., Cohen and Achache, 1990; Fejer and Scherliess, 1998; Lühr et al., 2004; Fejer et al., 2008; Rodrigues et al., 2015; Kumar et al., 2016; Zhou et al., 2018; Yizengaw and Groves, 2018]. CEJ studies can also be performed using Incoherent Scatter Radar (ISR) over Jicamarca or the mode that operates to determine E-region irregularities commonly known as the Jicamarca Unattended Long-Term Studies of Ionosphere and Atmosphere (JULIA) and similar coherent radar measurements in other longitude regions such as the Indian and Indonesian sectors [Patra et al., 2008, 2014]. For-example, Rodrigues et al. [2015] reported statistical results comparing C/NOFS Ion Velocity Meter (IVM) observations with 150 km echo drifts over the Peruvian sector during 2008-2009. While different sources of vertical drifts' measurements exist, it still remains a challenge to understand ionospheric dynamics and electrodynamics in some longitude regions with very limited information such as the African region and over the oceanic areas. In the context of radar and satellite measurements, the latter is attractive owing to the satellite's ability to sample all longitude sectors, providing measurements on global scale. The shortcoming of satellite measurements is the inability to provide continuous temporal variability of vertical drift data over a certain longitude sector, thus only providing 'snapshots', making its data applicable for long-term climatology studies. In absence of 'expensive' radar infrastructure, other ground-based instrumentation such as magnetometers provide EEJ/CEJ information and hence vertical plasma drifts [e.g., Anderson et al., 2002, 2004; Yizengaw et al., 2014; Habarulema et al., 2018], although this is mainly limited to local daytime. This paper is aimed at statistically comparing the CEJ occurrences identified from ground-based magnetometer and C/NOFS observations over the American and African sectors during 2008-2014. The motivations for performing this fairly detailed analysis are based on earlier studies which showed that ground-based and satellite observations sometimes do not agree in identifying the downward drifts during similar local times [e.g., Rodrigues et al., 2015] and to establish the

82 extent of agreement/disagreement based on local time. One of the implications of this  
83 study lies in the correct interpretation of results from models developed by combining  
84 both ground and satellite based observations to describe the equatorial electrodynamics.  
85 For event(s) analyses, variations in EEJ/CEJ provides insights into the variability of the  
86 equatorial ionization anomaly during geomagnetically disturbed conditions [Stolle *et al.*,  
87 2008; Venkatesh *et al.*, 2015], and is thus an important parameter to accurately describe in  
88 order to understand the evolution and/or drivers of space weather events. Therefore, when  
89 a space weather event occurs, it is important to first establish the original variability nature  
90 and/or magnitude of the eastward electric field in equatorial regions before attributing the  
91 resulting changes to solar wind-magnetosphere and ionosphere coupling processes since  
92 CEJ events can be present even during quiet conditions.

## 93 **2 C/NOFS and magnetometer data treatment**

94 Satellite and magnetometer data were analysed during geomagnetically quiet con-  
95 ditions based on the planetary Kp ( $K_p \leq 3$ ) index criterion. The Kp index data was down-  
96 loaded from [wdc.kugi.kyoto-u.ac.jp/kp/index.html](http://wdc.kugi.kyoto-u.ac.jp/kp/index.html). The in-situ equivalent vertical  $\mathbf{E} \times \mathbf{B}$   
97 drift data are estimated from the Ion Velocity Meter (IVM) drift measurements on-board  
98 C/NOFS satellite, averaged within the altitude range of 400-550 km [Stoneback *et al.*,  
99 2011, 2012; Yizengaw *et al.*, 2014; Rodrigues *et al.*, 2015] during 2008-2014. Due to the  
100 intention of directly comparing with magnetometer derived EEJ, it was necessary to limit  
101 the latitudinal coverage of satellite's data around the geomagnetic equator by constraining  
102 the latitude of observations to remain within the EEJ band. For this purpose, the latitude  
103 range used was  $\pm 4$  degrees around the geomagnetic equator and within a longitude range  
104 of  $\pm 8^\circ$  centered around the meridian of the pair of magnetometer stations [e.g., Dubazane  
105 and Habarulema, 2018; Habarulema *et al.*, 2018] for both African and American sectors.  
106 In an effort to minimize potential outliers associated with C/NOFS vertical ion plasma  
107 drift data within 400-550 km, we employed the median and scaled median absolute de-  
108 viation [e.g., Huber, 1981; Huber and Ronchetti, 2009] for each satellite track during the  
109 entire period (2008-2014) of analysis. This filtering method has been previously used in  
110 related analyses [e.g., Lomidze *et al.*, 2017; Dubazane and Habarulema, 2018; Habarulema  
111 *et al.*, 2018] and is demonstrated in Dubazane and Habarulema [2018] for C/NOFS satel-  
112 lite data treatment. After removing outliers, the C/NOFS data is averaged in 3 minutes  
113 intervals. For the EEJ/CEJ measurements, we used two pairs of ground-based magne-

114 tometers in both African and American sectors during the period of 2008-2014. Figure  
115 1 shows the locations of magnetometers that we used for this study. The geographic and  
116 geomagnetic coordinates are shown in Table 1 along with the exact locations and coun-  
117 try. The corrected geomagnetic coordinates [Gustafsson *et al.*, 1992] are obtained from  
118 geographic coordinates based on the International Geomagnetic Reference Field (IGRF)  
119 model for the Epoch year 2010. In the African sector, apart from AAE which is part of  
120 the INTERMAGNET (International Real-time Magnetic Observatory Network), the rest  
121 of the magnetometer stations are operated under the auspice of the AMBER (African  
122 Meridian and B-Field Education Research) project [Yizengaw and Moldwin, 2009; Yizen-  
123 gaw *et al.*, 2011]. The two pairs of magnetometer locations used in the Africa are Addis  
124 Ababa, AAE (9.0°N, 38.8°E) and Adigrat, ETHI (14.3°N, 39.5°E) for East African sec-  
125 tor; and Abuja, ABJA (10.5°N, 7.6°E) and Yaounde, CMRN (3.9°N, 11.5°E) for West  
126 African sector. All South American magnetometer stations in Table 1, form part of the  
127 LISN (Low Latitude Ionospheric Sensor Network) project [Valladares and Chau, 2012].  
128 These are Puerto Maldonado, PUER (12.6°S, 69.2°W) and Leticia, LETI (4.2°S, 69.9°W);  
129 and Alta Floresta, ALTA (9.9°S, 56.1°W) and Cuiaba, CUIB (15.6°S, 56.1°W). Magne-  
130 tometer data used in this study are freely available from <http://magnetometers.bc.edu/>,  
131 [www.intermagnet.org](http://www.intermagnet.org) and <http://lisn.igp.gob.pe/data/> for AMBER, INTERMAGNET and  
132 LISN networks respectively.

135 Each pair of magnetometer locations was used to compute the EEJ from the Earth's  
136 geomagnetic field's horizontal component following the established standard procedure  
137 done in many sources [e.g., Anderson *et al.*, 2002, 2004; Yizengaw *et al.*, 2012]. This pro-  
138 cedure is based on differencing the horizontal component measurements (after removing  
139 the average nighttime baseline value) of a magnetometer displaced by 6-9 degrees from  
140 the geomagnetic equator from the corresponding  $H$  values measured by the magnetome-  
141 ter at the equator. The estimated EEJ is a proxy of low latitude vertical  $\mathbf{E} \times \mathbf{B}$  drift [e.g.,  
142 Anderson *et al.*, 2004; Yizengaw *et al.*, 2011; Habarulema *et al.*, 2018]. Figure 2 shows  
143 local daytime changes in  $H$  component after removing the nightside (2300-0300 local  
144 time) baseline measured at the equator and off the equator, and the differences between  
145 the two representing the EEJ for randomly selected days over the American (PUER-LETI  
146 (23 November 2011) and ALTA-CUIB (28 October 2012)) and African (ABJA-CMRN (23  
147 January 2012) and AAE-ETHI (19 November 2008)) regions. Superimposed on the  $\Delta H$

133 **Table 1.** Geographic and geomagnetic coordinates of magnetometer stations used to estimate EEJ over the  
 134 American and African sectors in this study.

Location/country	Code	Source	Geographic coordinates		Geomagnetic coordinates	
			Latitude	Longitude	Latitude	Longitude
<b>African sector</b>						
Abuja (Nigeria)	ABJA	AMBER	10.5	7.6	-0.6	79.6
Yaounde (Cameroon)	CMRN	AMBER	3.9	11.5	-5.3	83.1
Addis Ababa (Ethiopia)	AAE	INTERMAGNET	9.0	38.8	0.2	110.5
Adigrat (Ethiopia)	ETHI	AMBER	14.3	39.5	6.0	111.1
<b>American sector</b>						
Puerto Maldonado (Peru)	PUER	LISN	-12.6	-69.2	0.0	2.0
Leticia (Brazil)	LETI	LISN	-4.2	-69.9	8.2	2.0
Alta Floresta (Brazil)	ALTA	LISN	-9.9	-56.1	0.8	15.2
Cuiaba (Brazil)	CUIB	LISN	-15.6	-56.1	-5.9	13.8

148 (nT) plots are the available vertical ion plasma drift values from C/NOFS satellite (simply  
 149 represented as vertical  $\mathbf{E} \times \mathbf{B}$  drift indicated as black dots).

150 In Figure 2, there are periods when both C/NOFS satellite and  $\Delta H$  (nT) data agree  
 151 in identifying either upward or downward vertical drifts. Noticeable differences are also  
 152 visible as in the case for Figure 2(b), bottom panel, where  $\Delta H$  (nT) was mostly negative  
 153 between 1300 and 1400 LT (corresponding to downward vertical drifts) while C/NOFS  
 154 observations show upward drifts or viceversa (see Figure 2(d) between 0900 and 1100 LT  
 155 for AAE on 19 November 2008). This highlights one of the reasons why we have decided  
 156 to statistically study the differences and similarities between these datasets in showing CEJ  
 157 occurrences.

### 158 **3 Results and discussion**

159 Due to the unusual extended solar minimum at the end of solar cycle 23 during  
 160 2008-2010 [e.g., *Chen et al.*, 2011; *Ezquer et al.*, 2014] when vertical  $\mathbf{E} \times \mathbf{B}$  drift did not  
 161 show expected direct relationship with solar activity [e.g., *Dubazane and Habarulema*,  
 162 2018; *Habarulema et al.*, 2018], the presentation of results is categorized into two peri-

163 ods of 2008-2010 and 2011-2014 respectively for both the American and African sectors.  
 164 This was however done only for the 69°W (American) and 38°E (African) longitude sec-  
 165 tors where 2008-2014 data were available; otherwise 2011-2014 datasets were analysed  
 166 for the 56°W (American) and 9°E (African) longitude sectors. A recent detailed inves-  
 167 tigation about CEJ occurrence with respect to different variables including solar activity  
 168 using average properties derived from CHAMP data during 2000-2010 reported more oc-  
 169 currence rates for low solar flux levels [Zhou *et al.*, 2018]. For direct comparisons, mag-  
 170 netometer derived  $\Delta H$  was only considered at epochs when C/NOFS data were available,  
 171 otherwise magnetometer data are extensively available. There were however few instances  
 172 where C/NOFS data were available with no corresponding magnetometer data and these  
 173 cases were also not included in the analysis. To identify CEJ occurrence, we have sim-  
 174 ply considered cases where C/NOFS vertical  $\mathbf{E} \times \mathbf{B}$  drift and  $\Delta H$  are negative (less than  
 175 zero), thus we do not have any threshold magnitude for each of these parameters. Fig-  
 176 ure 3 shows scatter plots of C/NOFS vertical  $\mathbf{E} \times \mathbf{B}$  drift against  $\Delta H$  for PUER and AAE  
 177 representing American and African sectors respectively. For the entire datasets, correla-  
 178 tion values of 0.54 and 0.50 were obtained between C/NOFS vertical  $\mathbf{E} \times \mathbf{B}$  drift and  $\Delta H$   
 179 for PUER and AAE, respectively. The derived  $\Delta H$  data from PUER-LETI pair of mag-  
 180 netometer stations is mostly available from 2009 and further contains significant data  
 181 gaps especially in 2010-2011, explaining the difference in data points displayed in scat-  
 182 ter plots of Figure 3 for PUER and AAE. The correlation values are comparable to ear-  
 183 lier results which reported values of 0.57 and 0.51 over Jicamarca [Habarulema *et al.*,  
 184 2018] and AAE [Dubazane and Habarulema, 2018], respectively between C/NOFS ver-  
 185 tical  $\mathbf{E} \times \mathbf{B}$  drift and  $\Delta H$ . The low correlation values are attributed to the altitude differ-  
 186 ences at which C/NOFS vertical  $\mathbf{E} \times \mathbf{B}$  drift and  $\Delta H$  are computed.  $\Delta H$  represents EEJ  
 187 which is typically in the E-region (about 110 km) while C/NOFS vertical ion plasma drift  
 188 (equivalent to vertical  $\mathbf{E} \times \mathbf{B}$  drift at 400 km) was estimated within an altitude range of  
 189 400-550 km. Furthermore, the variation of neutral wind velocity with respect to altitude  
 190 in low latitudes can alter ‘the ground magnetic perturbation a few degrees’ off the mag-  
 191 netic equator [Fambitakoye *et al.*, 1976; Fang *et al.*, 2008] and therefore contribute to the  
 192 differences between derived  $\Delta H$  and C/NOFS vertical  $\mathbf{E} \times \mathbf{B}$  drift observations. Figure 3  
 193 shows that the C/NOFS satellite and  $\Delta H$  observed more CEJ occurrence over the African  
 194 sector (AAE) compared to the American sector (PUER). Statistically, negative  $\mathbf{E} \times \mathbf{B}$  drift  
 195 ( $\Delta H$ ) values interpreted as CEJ events account for 36%(18%) for PUER (Figure 3(a)) and



196 75% (28%) over AAE (Figure 3(b)). With regard to C/NOFS satellite data, our results  
197 are in agreement with previous seasonal analysis based on IVM data from 2009/2010 to  
198 2013 that showed vertical  $\mathbf{E} \times \mathbf{B}$  drift values in the African sector to be dominated by neg-  
199 ative values (with a slight exception for September Equinox) compared to the American  
200 sector [Yizengaw *et al.*, 2014; Yizengaw and Groves, 2018]. In Figure 3(b), an attempt to  
201 derive a direct relationship between the two parameters shows that a significantly large  
202 value of positive  $\Delta H$  is required for an upward vertical drift at C/NOFS satellite altitude  
203 in the African sector. In both sectors, C/NOFS satellite observes more downward drifts  
204 than the magnetometer method, although a higher occurrence rate is more pronounced in  
205 the African sector. Being at a low inclination ( $13^\circ$ ) angle within an elliptical orbit, the  
206 C/NOFS satellite provides relatively detailed information within low/equatorial latitudes at  
207 all longitude sectors than other LEO satellites such as the ones in near polar orbit.

### 208 **3.1 Local time occurrence of CEJ over the American sector**

209 We have analysed CEJ occurrences by looking at the number of times when the  
210 C/NOFS vertical  $\mathbf{E} \times \mathbf{B}$  drift and  $\Delta H$  were negative within hourly bins (07-08 LT, 08-  
211 09 LT, ..., 16-17 LT) during magnetically quiet conditions ( $K_p \leq 3$ ). Figure 4 shows diur-  
212 nal CEJ occurrences (expressed as a percentage of total number of data points within an  
213 hour) as observed by C/NOFS and magnetometer derived  $\Delta H$  data over (a) PUER ( $12.6^\circ\text{S}$ ,  
214  $69.2^\circ\text{W}$ ) and (b) ALTA ( $9.9^\circ\text{S}$ ,  $56.1^\circ\text{W}$ ) within the American sector. C/NOFS and  $\Delta H$   
215 CEJ identification results are plotted in blue and green bars respectively. In both cases, the  
216 right-hand side of each subplot indicates the total number of data points (plotted as black  
217 dots) when coincidental observations were obtained simultaneously from C/NOFS and  $\Delta H$   
218 measurements. ALTA had magnetometer data for simultaneous analyses with C/NOFS  
219 data during 2011-2014. Otherwise results over PUER (a) correspond to CEJ occurrence  
220 as detected by C/NOFS and  $\Delta H$  observations for the periods of 2008-2010 and 2011-  
221 2014 respectively. In general, both C/NOFS and magnetometer data show that CEJ usu-  
222 ally occurs during morning and evening times, a result similar to previous findings over  
223 the African and American sectors based on 2009 magnetometer data [Rabiu *et al.*, 2017].  
224 The main difference from Figure 4 is that C/NOFS data shows more cases in CEJ occur-  
225 rences than magnetometer data in the afternoon hours for both PUER and ALTA. While  
226 this is mostly evident, a specific example in Figure 4(b) is for the case of 1500-1600 LT  
227 where CEJ occurrence identified by C/NOFS data is more than double the corresponding



228 result for magnetometer observations. Using radar and C/NOFS datasets during 2008-2009  
229 over Jicamarca, *Rodrigues et al.* [2015] observed that the C/NOFS afternoon downward  
230 vertical drift values did not feature in the 150 km echoes, which by inference may be true  
231 for  $\Delta H$  as both JULIA and  $\Delta H$  observations are all approximately within the E- region  
232 [e.g., *Anderson et al.*, 2004]. In particular, we note that the percentage CEJ occurrences  
233 from magnetometer derived  $\Delta H$  is either less than 20% or absent during local times 1000-  
234 1600 LT for both 2008-2010 and 2011-2014. In fact, this observation can be extended to  
235 start from 0900 LT, with exception of PUER results during 2008-2010. While the same  
236 consistency is not visible for C/NOFS observations, CEJ identification occurrences which  
237 are less than 20% can be noticed during 1200-1500 LT (2008-2010) and 1000-1300 LT  
238 (2011-2014) over PUER and ALTA respectively. Based on the criteria defined in *Alex and*  
239 *Mukherjee* [2001] while analysing magnetometer data over the African and Indian sec-  
240 tors, *Chandrasekhar et al.* [2017] reported high CEJ occurrence rate during morning hours  
241 (0700-1000 LT) followed by evening (1500-1800 LT), afternoon (1200-1500 LT) and lastly  
242 noon hours (1000-1200 LT). This is well reflected in Figure 4 for both PUER and ALTA  
243 (longitude separation of 13 degrees) for C/NOFS and magnetometer data although the per-  
244 centage CEJ occurrence rate may be different in some cases. *Zhou et al.* [2018] showed  
245 that CEJ occurrence rate reduces to about 4% at noon. Differences in CEJ occurrence rate  
246 between SWARM satellite and magnetometer observations have been recently reported  
247 [*Soares et al.*, 2018], but their ‘qualitative agreement’ was emphasized. Morning CEJ  
248 occurrence in  $\Delta H$  is therefore dominant for both PUER (69.2°W longitude) and ALTA  
249 (56.1°W longitude). For the Brazilian sector where ALTA lies, our results are consistent  
250 with findings in *Venkatesh et al.* [2015] and *Soares et al.* [2018]. Statistically, C/NOFS  
251 data are in agreement with magnetometer observations in showing predominantly morn-  
252 ing CEJ occurrence with about 80% and 48% for PUER during 2008-2010 and 2011-2014  
253 respectively; and 50% for ALTA in 2011-2014 during 0700-1000 LT. The rest of the CEJ  
254 occurrence rate is spread over other local times, but with afternoon CEJ occurrence be-  
255 ing more predominant from C/NOFS observations. The presence of afternoon downward  
256 vertical drifts in C/NOFS vertical ion plasma drift data when the 150 km echo drifts from  
257 the JULIA experiment showed largely upward drifts over Jicamarca has been reported [*Ro-*  
258 *drigues et al.*, 2015]. Due to the altitude of the C/NOFS satellite, these afternoon down-  
259 ward drifts (CEJ in this case) were attributed to the possibility of increased magnitude  
260 of semidiurnal tides in the topside ionosphere [*Stoneback et al.*, 2011; *Rodrigues et al.*,

261 2015]. With respect to local time, this quiet time analysis shows that C/NOFS satellite ob-  
262 serves more CEJ events than magnetometer observations by average of about 20% over  
263 the American sector, despite both datasets showing similar trends in CEJ identification.  
264 The result of the same trend from C/NOFS data at all local times with magnetometer data  
265 is important as satellite data augment the modelling approaches of vertical  $\mathbf{E} \times \mathbf{B}$  drift  
266 on both regional and global scales. Regarding the existence of CEJs during different ge-  
267 omagnetic conditions, *Zhou et al.* [2018] showed that the CEJ occurrence rate increases  
268 with increase in geomagnetic activity. Nevertheless, there is significant CEJ occurrence  
269 during quiet conditions, and therefore, when a space weather event occurs, detailed inves-  
270 tigation should be done to first understand the behaviour of the eastward electric field in  
271 low/equatorial latitudes before concluding about the effects of disturbed dynamo electric  
272 fields. This has the potential to assist in future development of improved vertical  $\mathbf{E} \times \mathbf{B}$   
273 drift models for accurate specification of space weather effects and their variability on the  
274 ionosphere. A brief summary of suggested mechanisms (and relevant literature references)  
275 responsible for occurrence of CEJ is presented in *Zhou et al.* [2018].

### 276 3.2 Local time occurrence of CEJ over the African sector

277 Figure 5 is similar to Figure 4, but for (a) AAE (9.0°N, 38.8°E) and (b) ABJA (10.5°N,  
278 7.6°E) in the African sector. Analyses over AAE (Figure 5(a)) are for CEJ occurrences  
279 obtained from C/NOFS and magnetometer  $\Delta H$  data for 2008-2010 and 2011-2014 respec-  
280 tively during local daytime (0700-1700 LT). Similar to Figure 4, the right handside repre-  
281 sents the total number of data points used to compute the percentage CEJ occurrence (left  
282 handside) during one hour interval.

283 C/NOFS satellite observations are consistent in identifying higher CEJ occurrences  
284 than ground-based magnetometer  $\Delta H$  data over both AAE and ABJA (when data are avail-  
285 able). However the rate of CEJ occurrence over the African sector is higher than in the  
286 American sector as observed from both C/NOFS satellite and magnetometer measure-  
287 ments. As an example, we shall be comparing AAE and PUER results, since they both  
288 have information for 2008-2014. Based on this example, it is estimated that CEJ occur-  
289 rences averaged over all local times were about 30% and 10% higher over AAE (African  
290 sector) than PUER (American sector) for C/NOFS satellite and magnetometer observa-  
291 tions respectively. The difference of 10% is even lower than the reported 40% over the  
292 Indian sector within a longitudinal difference of 15° based on magnetometer data [*Chan-*

293 *drasekhar et al.*, 2017]. Apart from differences in the local time occurrence of CEJ, there  
294 is little or no average statistical difference in CEJ occurrence rate with respect to different  
295 solar activity periods (2008-2010 and 2011-2014) for both C/NOFS and  $\Delta H$  results. Using  
296 magnetometer data in 2009, it was reported that the African sector exhibited more CEJ  
297 occurrence rate than the American sector [*Rabiu et al.*, 2017], and this also reflected in the  
298 CEJ seasonal dependence analysis as we shall show later. This appears to be the case for  
299 an extended period of time given that we have performed a statistical analysis for at least  
300 6 years. Over AAE, both datasets show high frequency of CEJ occurrence rate during the  
301 morning and afternoon/evening hours, a result similar to South American sector results  
302 with respect to local time trends of CEJ occurrence. Once again, C/NOFS satellite obser-  
303 vations largely exhibit more CEJ occurrences than magnetometer data. Concerning earlier  
304 satellite CEJ studies, *Cohen and Achache* [1990] used MAGSAT data (average altitude  
305 of 400 km) and reported dominant CEJ in morning hours compared to dusk hours, but  
306 added a caveat about the procedure applied that could have influenced the interpretation  
307 of results. Over both African and American sectors, the cases where CEJ events are not  
308 captured in magnetometer data may not necessarily mean that they are absent, and should  
309 be understood within the framework of having limited both magnetometer and C/NOFS  
310 satellite data simultaneously available and yet the latter may be limited due to its orbit pe-  
311 riod. However, fewer CEJ occurrences during some day-time hours (0900-1100 LT) have  
312 previously been reported in the Indian and African sectors [*Alex and Mukherjee*, 2001]  
313 and attributed to increased eastward electric and high gradients in ionospheric conduc-  
314 tivity during these local times. Here, we re-emphasize that there is more CEJ occurrence  
315 rate from magnetometer data in the African sector compared to the American sector. This  
316 could be linked to the the longitudinal differences where the magnitude of vertical drift  
317 velocity that has been shown to be stronger in the American sector [*Yizengaw et al.*, 2012].

### 318 **3.3 Agreement of C/NOFS and $\Delta H$ observations in CEJ identification**

319 Figure 6 demonstrates the percentage agreement between C/NOFS satellite and  $\Delta H$   
320 data in CEJ identification for (a) American sector (PUER (panels I and II) and ALTA  
321 (panel III)), and (b) African sector represented by AAE (panels I and II) and ABJA (panel  
322 III). In all subplots/panels, the total number of data points within each hour range is plot-  
323 ted (on the right handside y-axis) as black dots. In Figure 6, the agreement for the two  
324 datasets is presented separately during the periods of 2008-2010 and 2011-2014. Although

325 the dataset may not be identical because of the amount of data for each individual lon-  
326 gitude sector, we observe that the CEJ occurrence rate is different between the African  
327 and American sectors, even within each sector itself. It has been reported that the CEJ  
328 occurrence may be localized even for smaller longitude separation of about 1 hour [*Chan-*  
329 *drasekhar et al., 2017*], owing to different changes in neutral winds and local electrody-  
330 namics [*Rangarajan and Rastogi, 1993; Alex and Mukherjee, 2001, and references therein*].  
331 To a large extent, the diurnal variability of the percentage agreement between C/NOFS  
332 satellite and  $\Delta H$  data in identifying CEJ events follows very closely a similar trend of the  
333 CEJ occurrence rate as detected by magnetometer  $\Delta H$  data. This is clearly visible when  
334 comparing  $\Delta H$  plots in Figures 4 and 5 with Figure 6(a) and Figure 6(b) for the Ameri-  
335 can and African sectors, respectively. This implies that most of the CEJ events observed  
336 in  $\Delta H$  data were also captured by the C/NOFS satellite. Up to date, causes of CEJ con-  
337 tinue to be a major research subject since their identification by *Gouin [1962]*. Figure  
338 6 also shows that CEJ occurrences are dominant in morning and evening hours and this  
339 has been documented by several experimental and theoretical studies in different longi-  
340 tude sectors [e.g., *Marriott et al., 1979; Hanuise et al., 1983; Alex and Mukherjee, 2001;*  
341 *Chandrasekhar et al., 2017; Rabiou et al., 2017, and references therein*]. It has been demon-  
342 strated that contribution of semi diurnal tides exhibiting modes of different magnitudes  
343 to the electric field plays a role in the occurrence of CEJs in morning and evening local  
344 times over the equator [e.g., *Marriott et al., 1979; Hanuise et al., 1983; Alex and Mukher-*  
345 *jee, 2001*]. *Stening et al. [1996]* argued that CEJ events (termed as reverse electrojet in  
346 their paper) are possibly caused by global tidal dynamics with linkage to stratospheric  
347 warming. These authors showed that high latitude changes in mean zonal winds within  
348 the altitudes 90-100 km were associated with stratospheric warming which will later in-  
349 fluence the circulation of global tides thereby contributing to driving of CEJ events. This  
350 interpretation was mainly plausible for CEJ events which occurred in northern (southern)  
351 winter (summer) hemispheres. *Raghavarao and Anandarao [1980]* showed that the uplift-  
352 ment of ions by vertical upward winds of sufficient magnitudes (e.g. 13 m/s) can lead to  
353 the cancellation and/or reversing of the upward polarization electric field that gives rise to  
354 eastward electric field during local daytime. The origin of these vertical winds could be  
355 gravity waves that have been shown to have a significant effect in modifying the electrojet  
356 within altitudes of 110-150 km [*Anandarao, 1976*]. It is established that the solar termina-  
357 tor contributes to launching of atmospheric gravity waves [e.g., *Beer, 1978; Forbes et al.,*

2008]. There are therefore a number of suggested dynamic and electrodynamic processes that could contribute to CEJ occurrences, and it is not feasible to point out the dominant mechanism(s) in a statistical study of this nature. Our main emphasis was to establish the agreement/disagreement between C/NOFS satellite and magnetometer data in observing these CEJ occurrences which would later be useful in deciding to combine these datasets for modelling purposes especially that satellite data is attractive for longitudinal observations.

#### 4 Seasonal dependence of CEJ

For American and African sectors, both C/NOFS satellite vertical ion plasma drift and  $\Delta H$  observations from 2011-2014 (which had substantial amount of data) were categorised according to seasons representing Summer (December, January, February), Autumn (March-May), Winter (June-August) and Spring (September-November). The seasonal analysis was limited to 2011-2014 due to substantial missing  $\Delta H$  data over PUER prior to 2011 to avoid potential cases of generating 'statistically biased' results. Figure 3 shows that PUER had fewer number of data points (650) compared to AAE (2037), and a detailed difference during 2008-2010 can be seen in the first two panels of Figures 4(a) and 5(a) for both sectors. Figure 7 shows the percentage seasonal occurrence of CEJ for (a) PUER (12.6°S, 69.2°W), and (b) AAE (9.0°N, 38.8°E) representing the American and African sectors respectively. The red and blue bars represent CEJ occurrence observed from  $\Delta H$  and C/NOFS satellite data respectively.

In all seasons, there are more CEJ events recorded by C/NOFS satellite compared to magnetometer observations. The CEJ occurrence rate is present up to 60% (for C/NOFS satellite data) in the American sector and at all local day times in the African sector as revealed by C/NOFS satellite and magnetometer measurements during the Winter season. There are times when C/NOFS satellite data only show CEJ events with no single CEJ occurrence detected in magnetometer  $\Delta H$  data for most of the season. This is more prominent in the American sector especially in Summer between 1100-1500 LT (Figure 7(a), panel I) and Spring from 1100-1700 LT (see panel IV, Figure 7(a)). C/NOFS satellite observations show the CEJ occurrence rate in both sectors at all times (except at 1100-1200 LT over the American sector) with more events over the African sector in Winter. CEJ occurrence during the northern hemisphere Winter season has been previously linked to sudden stratospheric warming [Stening *et al.*, 1996]. In Figure 7(a)-(b), panel I, there

390 is a significant occurrence of CEJs for both American and African sectors especially for  
391 C/NOFS satellite observations. C/NOFS satellite observes CEJ occurrence of more than  
392 60% in both African and American sectors, at almost all times (apart from 0900-1100  
393 LT in the American sector). Broadly speaking, CEJ occurrences are more prominent in  
394 the African sector than the American sector during all seasons, a result that agrees well  
395 with previous studies such as the one of *Rabiu et al.* [2017] which analyzed geomagnetic  
396 data over Huancayo (75.22°W, 12.07°S) and AAE in 2009. *Rabiu et al.* [2017] showed  
397 that CEJ events were consistently present at all seasons over the African sector. In fact,  
398 their monthly statistics based on magnetometer data showed that morning CEJs were a  
399 common feature up to 100% over AAE apart from months of June, November and De-  
400 cember in 2009. Seasonally, we have shown that higher differences in CEJ occurrence rate  
401 between the African and American sectors for both C/NOFS satellite and magnetometer  
402 observations is in Southern Hemisphere Winter (June-August), a finding similar to results  
403 reported in *Soares et al.* [2018], and attributed to the dominance of wave-4 pattern. This  
404 is also consistent with the most recent comprehensive climatological analysis based on  
405 CHAMP satellite data which showed that CEJ occurrence rate peaks around July-August  
406 [*Zhou et al.*, 2018]. Previous seasonal analyses of vertical  $\mathbf{E} \times \mathbf{B}$  drift in different longi-  
407 tude sectors revealed that the C/NOFS satellite observes more downward drifts or nega-  
408 tive  $\mathbf{E} \times \mathbf{B}$  drift values ( corresponding to CEJ in this study) in the African sector than the  
409 American sector [*Yizengaw et al.*, 2014; *Yizengaw and Groves*, 2018]. These authors fur-  
410 ther showed that December and June solstices exhibit largely negative C/NOFS vertical  
411  $\mathbf{E} \times \mathbf{B}$  drift in the African sector (AAE) which agrees with our Winter and Summer sea-  
412 sons analyses. For both December and June solstice as well as March/September equinox  
413 months, *Yizengaw and Groves* [2018] reported average upward/positive vertical  $\mathbf{E} \times \mathbf{B}$  drift  
414 variability from C/NOFS satellite observations. Conditions favourable for CEJ occurrence  
415 would have to involve generation of reverse current with magnitudes greater than the back-  
416 ground eastward electric field over the equator. It is remarked that locations with strong  
417 EEJ record the lowest CEJ occurrence rate as is the case with this study. It is known that  
418 the American sector exhibits strong EEJ strength [e.g., *Yizengaw et al.*, 2014; *Rabiu et al.*,  
419 2017] compared to the African sector. To understand the relative contribution of differ-  
420 ent physical processes such as upward vertical winds possibly related to gravity waves  
421 [*Raghavarao and Anandarao*, 1980] and tidal effects [*Stening et al.*, 1996], extensive neu-  
422 tral wind data is necessary in both sectors. This is an issue for further investigations when

423 data becomes available, especially in the African sector. While other sources make a sim-  
424 ilar/related observation, it is particularly useful to establish that C/NOFS satellite data are  
425 consistent with magnetometer and other ground-based data in identifying the CEJ seasonal  
426 dependence. To our knowledge, this is the first study that has shown this statistical confir-  
427 mation using C/NOFS satellite data moreover in both African and American sectors.

## 428 5 Conclusions

429 We have presented statistical analyses of CEJ occurrences based on ground-based  
430 magnetometer and C/NOFS satellite observations over the South American and African  
431 regions during 2008-2014. Due to the extended deep solar minimum from 2008-2009, we  
432 performed the analysis by considering periods 2008-2010 and 2011-2014 separately. On  
433 average, we found no significant difference in CEJ occurrence rate during the extremely  
434 low solar activity period of 2008-2010 compared to 2011-2014 in both African and Amer-  
435 ican sectors, an observation that is found for both satellite and magnetometer measure-  
436 ments. However, the frequency of CEJ occurrence was found to be greater in C/NOFS  
437 satellite data than magnetometer observations in the African and American sectors. The  
438 interpretation of this difference partly lies in the fact that the EEJ/CEJ derived from mag-  
439 netometer data is a representation of electric current system in the ionospheric E region  
440 (90-110 km) which is basically over 300 km below the altitude of the C/NOFS satel-  
441 lite. In general, we have observed that CEJ occurrences are more prevalent in the local  
442 morning and afternoon/evening, a result that agrees with existing literature [e.g., *Alex and*  
443 *Mukherjee*, 2001; *Venkatesh et al.*, 2015; *Chandrasekhar et al.*, 2017; *Rabiu et al.*, 2017;  
444 *Soares et al.*, 2018]. The C/NOFS satellite data found significant CEJ occurrence in the  
445 afternoon hours compared to magnetometer observations over both American and African  
446 sectors. For the American sector, a similar observation has been reported while compar-  
447 ing C/NOFS satellite and 150 km echo drifts data from Jicamarca [*Rodrigues et al.*, 2015],  
448 which was interpreted to be a result of increased magnitudes of the semi-diurnal tides in-  
449 fluence in the topside ionosphere [*Stoneback et al.*, 2011]. This is the first detailed statis-  
450 tical analysis dedicated to CEJ occurrence as observed by the C/NOFS satellite over the  
451 African sector. However there exists studies that look at general trends of the ionospheric  
452 electrodynamics using various data sources including C/NOFS satellite data [*Yizengaw*  
453 *et al.*, 2011, 2014]. This study is therefore particularly relevant in interpreting results gen-  
454 erated by ionospheric electrodynamics models developed by combining ground-based and



455 satellite observations given that the latter is attractive in regions inaccessible for instru-  
456 mentation deployment such as over the oceans.

### 457 **Acknowledgments**

458 Data for the C/NOFS satellite was obtained from <http://spdf.gsfc.nasa.gov/pub/data/cnofs/cindi/>.  
459 The C/NOFS mission is supported by the Air Force Research Laboratory, the Depart-  
460 ment of Defense Space Test Program, the National Aeronautics and Space Administration  
461 (NASA), the Naval Research Laboratory, and the Aerospace Corporation. Magnetome-  
462 ter data was obtained from the AMBER (<http://magnetometers.bc.edu/>), INTERMAGNET  
463 ([www.intermagnet.org](http://www.intermagnet.org)) and LISN (<http://lisn.igp.gob.pe/data/>) networks. All these data are  
464 freely available. The authors thank the AMBER and SAMBA teams for the magnetometer  
465 data. AMBER is operated by Boston College and funded by NASA and AFOSR. Different  
466 national institutes which support collected geomagnetic data are acknowledged. Thanks to  
467 INTERMAGNET for promoting high standards of magnetic observatory practice. LISN  
468 is a project led by the University of Texas at Dallas in collaboration with the Geophys-  
469 ical Institute of Peru, and other institutions that provide information in benefit of the sci-  
470 entific community. This work is based on the research supported in part by the National  
471 Research Foundation of South Africa (Grant Number 105778) and opinions, findings and  
472 conclusions or recommendations expressed in this paper are of the author(s), and the NRF  
473 accepts no liability whatsoever in this regard. The work by GL and MBM was supported  
474 by NSF OISE 1459911 and AGS 1450512. EY's work has been partially supported by the  
475 Aerospace Corporation SERPA program.

### 476 **References**

- 477 Alex, S., and S. Mukherjee (2001), Local time dependence of the equatorial counter elec-  
478 trojet effect in a narrow longitudinal belt, *Earth Planets Space*, *53*, 1151–1161.
- 479 Anandarao, B. G. (1976), Effects of gravity wave winds and wind shears on equatorial  
480 electrojet, *Geophys. Res. Lett.*, *3*(9), 545–548.
- 481 Anderson, D., A. Anghel, K. Yumoto, M. Ishitsuka, and E. Kudeki (2002), Es-  
482 timating daytime vertical E×B drift velocities in the equatorial F-region us-  
483 ing ground-based magnetometer observations, *Geophys. Res. Lett.*, *29*(12), 1596,  
484 doi:10.1029/2001GL014562.

- 485 Anderson, D., A. Anghel, J. Chau, and O. Veliz (2004), Daytime vertical  $E \times B$  drift ve-  
486 locities inferred from ground-based magnetometer observations at low latitudes, *Space*  
487 *Weather*, 2(S11001), doi:10.1029/2004SW000095.
- 488 Beer, T. (1978), On atmospheric wave generation by the terminator, *Planetary and Space*  
489 *Science*, 26(2), 185–188.
- 490 Chandrasekhar, N. P., R. K. Archana, N. Nagarajan and K. Arora (2017), Variability of  
491 equatorial counter electrojet signatures in the Indian region, *Journal of Geophysical Re-*  
492 *search, Space Physics*, 122, 2185–2201, doi:10.1002/2016JA022904.
- 493 Chen, Y., L. Liu and W. Wan (2011), Does the F10.7 index correctly describe solar EUV  
494 flux during the deep solar minimum of 2007-2009?, *Journal of Geophysical Research*,  
495 116(A04304), doi:10.1029/2010JA016301.
- 496 Cohen, Y., and J. Achache (1990), New Global Vector Magnetic Anomaly Maps Derived  
497 From Magsat Data, *J. Geophys. Res.*, 95(B7), 10783–10800.
- 498 Dubazane, M. B., and J. B. Habarulema (2018), An empirical Model of vertical Plasma  
499 drift over the African sector, *Space Weather*, 16, 619–635.
- 500 Ezquer, R. G., J. L. López, L. A. Scidá, M. A. Cabrera, B. Zolesi, C. Bianchi, M. Pez-  
501 zopane, E. Zuccheretti, and M. Mosert (2014), Behaviour of ionospheric magnitudes  
502 of F2 region over Tucumán during a deep solar minimum and comparison with the IRI  
503 2012 model predictions, *Journal of Atmospheric and Solar-Terrestrial Physics*, 107, 89–  
504 98, doi:http://dx.doi.org/10.1016/j.jastp.2013.11.010.
- 505 Fambitakoye, O., P. N. Mayaud, and A. D. Richmond (1976), Equatorial elec-  
506 trojet and regular daily variation  $S_R$  - III. Comparison of observations with a  
507 physical model, *Journal of Atmospheric and Terrestrial Physics*, 38(2), 113–121  
508 [https://doi.org/10.1016/0021-9169\(76\)90118-5](https://doi.org/10.1016/0021-9169(76)90118-5).
- 509 Fang, T. W., A. D. Richmond, J. Y. Liu and A. Maute (2008), Wind dynamo effects  
510 on ground magnetic perturbations and vertical drifts, *J. Geophys. Res. Space Physics*,  
511 113(A11313), doi:10.1029/2008JA013513.
- 512 Fejer, B. G., J. W. Jensen, and S. -Y. Su (2008), Quiet time equatorial F region verti-  
513 cal plasma drift model derived from ROCSAT-1 observations, *J. Geophys. Res. Space*  
514 *Physics*, 113(A05304), doi:10.1029/2007JA012801.
- 515 Fejer, B. G., and L. Scherliess (1998), Mid- and low-latitude prompt ionospheric zonal  
516 plasma drifts, *Geophys. Res. Lett.*, 25(16), 3071–3074.

- 517 Forbes, J. M., S. L. Bruinsma, Y. Miyoshi, and H. Fujiwara (2008), A solar terminator  
518 wave in thermosphere neutral densities measured by the CHAMP satellite, *Geophys.*  
519 *Res. Lett.*, *35*, L14802, doi:10.1029/2008GL034075.
- 520 Gouin, G. (1962) Reversal of the magnetic daily variation at Addis Ababa, *Nature*, *193*,  
521 1145–1146.
- 522 Gustafsson, G., N. E. Papitashvili, and V. O. Papitashvili (1992), A Revised Corrected  
523 Geomagnetic Coordinate System for Epochs 1985 and 1990, *J. Atmos. Terr. Phys.*, *54*,  
524 1609–1631.
- 525 Habarulema, J. B., Dubazane, M. B. Z. T. Katamzi-Joseph, E. Yizengaw, M. B. Moldwin  
526 and J. C. Uwahoro (2018), Long-term estimation of diurnal vertical  $\mathbf{E} \times \mathbf{B}$  drift ve-  
527 locities using C/NOFS and ground-based magnetometer observations, *J. Geophys. Res.*  
528 *Space Physics*, (123), 6996–7010.
- 529 Hanuise, C., C. Mazaudier, P. Vila, M. Blanc and M. Crochet (1983), Global dynamo sim-  
530 ulation of ionospheric currents and their connection with the equatorial electrojet and  
531 counter-electrojet: A case study, *J. Geophys. Res.*, *88*(A1), 253–270.
- 532 Huber, P. J (1981), Robust Statistics, *John Wiley & Sons*, New York, USA.
- 533 Huber, P. J, and E. M. Ronchetti (2009), Robust Statistics: Second Edition, *John Wiley &*  
534 *Sons*, New York, USA.
- 535 Kikuchi, T., H. Lühr, K. Schlegel, H. Tachihara, M. Shinohara and T. -I. Kitamura (2000),  
536 Penetration of auroral electric fields to the equator during a substorm, *J. Geophys. Res.*,  
537 *105*(A10), 23251–23261.
- 538 Kumar, S., B. Veenadhari, S. Tulasi Ram, S.-Y. Su, and T. Kikuchi (2016), Possible rela-  
539 tionship between the equatorial electrojet (EEJ) and daytime vertical  $\mathbf{E} \times \mathbf{B}$  drift veloc-  
540 ities in F region from ROCSAT observations, *Advances in Space Research*, *58*, 1168–  
541 1176, <http://dx.doi.org/10.1016/j.asr.2016.06.009>.
- 542 Lomidze, L., D. J. Knudsen, J. Burchill, A. Kouznetsov, and S. C. Buchert (2017), Cal-  
543 ibration and Validation of Swarm Plasma Densities and Electron Temperatures Using  
544 Ground-Based Radars and Satellite Radio-Occultation Measurements, *Radio Science*,  
545 doi: 10.1002/2017RS006415.
- 546 Lühr, H., S. Maus, and M. Rother (2004), Noon-time equatorial electrojet: Its spatial  
547 features as determined by the CHAMP Ősatellite, *J. Geophys. Res. Space Physics*,  
548 *109*(A01306), doi:10.1029/2002JA009656.

- 549 Manoj, C., H. Lühr, S. Maus, and N. Nagarajan (2006), Evidence for short spatial correla-  
550 tion lengths of the noontime equatorial electrojet inferred from a comparison of satellite  
551 and ground magnetic data, *Journal of Geophysical Research: Space Physics*, *111*(A11),  
552 doi:10.1029/2006JA011855.
- 553 Marriott, R. T., A. D. Richmond, and S. V. Venkateswaran (1979), The Quiet-Time Equa-  
554 torial Electrojet and Counter-Electrojet, *J. Geomag. Geoelectr.*, *31*, 311–340.
- 555 Maute, A., A. D. Richmond and R. G. Roble (2012), Sources of low-latitude ionospheric  
556  $\mathbf{E} \times \mathbf{B}$  drifts and their variability, *J. Geophys. Res. Space Physics*, *117*(A06312), doi:  
557 10.1029/2011JA017502.
- 558 Mayaud, P. N. (1977), The equatorial counter-electrojet - a review of its geomagnetic  
559 aspects, *Journal of Atmospheric and Terrestrial Physics*, *39*(9-10), 1055–1070, doi:  
560 [https://doi.org/10.1016/0021-9169\(77\)90014-9](https://doi.org/10.1016/0021-9169(77)90014-9).
- 561 Patra, A. K., T. Yokoyama, Y. Otsuka, and M. Yamamoto (2008), Daytime 150 km echoes  
562 observed with the Equatorial Atmosphere Radar in Indonesia: First results, *Geophys.*  
563 *Res. Lett.*, *119*(5), 3777–3788, doi:10.1029/2007GL033130.
- 564 Patra, A. K., P. P. Chaitanya, Y. Otsuka, T. Yokoyama, M. Yamamoto, R. A. Stoneback,  
565 and R. A. Heelis (2014), Vertical  $\mathbf{E} \times \mathbf{B}$  drifts from radar and C/NOFS observations in  
566 the Indian and Indonesian sectors: Consistency of observations and model, *J. Geophys.*  
567 *Res. Space Physics*, *119*(5), 3777–3788, doi:10.1002/2013JA019732.
- 568 Rabiú, A. B., O. O. Folarin, T. Uozumi, N. S. A. Hamid, and A. Yoshikawa (2017), Lon-  
569 gitudinal variation of equatorial electrojet and the occurrence of its counter electrojet,  
570 *Annales Geophysicae*, *35*, 535–545, doi:10.5194/angeo-35-535-2017.
- 571 Rangarajan, G. K., and R. G. Rastogi (1993), Longitudinal Difference in Magnetic Field  
572 Variations Associated with Quiet Day Counter Electrojet, *J. Geomag. Geoelectr.*, *45* (8),  
573 649–656.
- 574 Rastogi, R. G. (1974), Westward equatorial electrojet during daytime hours, *J. Geophys.*  
575 *Res.*, *79* (10), 1503–1512.
- 576 Rastogi, R. G. (1974), Lunar effects in the counter electrojet near the magnetic  
577 equator, *Journal of Atmospheric and Terrestrial Physics*, *36*(1), 167–170, doi:  
578 [https://doi.org/10.1016/0021-9169\(74\)90074-9](https://doi.org/10.1016/0021-9169(74)90074-9).
- 579 Raghavarao, R., and B. G. Anandarao (1980), Vertical winds as a plausible cause for  
580 equatorial counter electrojet, *Geophysical Research Letters*, *7*(5), 357–360.

- 581 Rodrigues, F. S., J. M. Smith, M. Milla, and R. A. Stoneback (2015), Daytime ionospheric  
582 equatorial vertical drifts during the 2008-2009 extreme solar minimum, *J. Geophys. Res.*  
583 *Space Physics*, *120*, 1452–1459, doi:10.1002/2014JA020478.
- 584 Singh, D., S. Gurubaran, and M. He (2018), Evidence for the influence of DE3 tide on the  
585 occurrence of equatorial counter electrojet, *Geophys. Res. Lett.*, *45*, 2145–2150.
- 586 Stening, R. J., C. E. Meek, and A. H. Manson (1996), Upper atmosphere wind systems  
587 during reverse equatorial electrojet events, *Geophys. Res. Lett.*, *23*(22), 3243–3246.
- 588 Stolle, C., C. Manoj, H. Lühr, S. Maus, and P. Alken (2008), Estimating the daytime  
589 Equatorial Ionization Anomaly strength from electric field proxies, *J. Geophys. Res.*,  
590 *113*(A09310), doi:10.1029/2007JA012781.
- 591 Soares, G., Y. Yamazaki, J. Matzka, K. Pinheiro, A. Morschhauser, A. Stolle, and P. Alken  
592 (2018), Equatorial counter electrojet longitudinal and seasonal variability in the Ameri-  
593 can sector, *J. Geophys. Res. Space Physics*, *123*, 9906-9920.
- 594 Stoneback, R., R. Heelis, A. Burrell, W. Coley, B. G. Fejer, and E. Pacheco (2011),  
595 Observations of quiet time vertical ion drift in the equatorial ionosphere during the  
596 solar minimum period of 2009, *J. Geophys. Res. Space Physics*, *116*(A12327), doi:  
597 10.1029/2011JA016712.
- 598 Stoneback, R. A., R. L. Davidson, and R. L. Heelis (2012), Ion drift meter calibration  
599 and photoemission correction for the C/NOFS satellite, *J. Geophys. Res. Space Physics*,  
600 *117*(A08323), doi:10.1029/2012JA017636.
- 601 Siddiqui, T. A., A. Maute, N. Pedatella, Y. Yamazaki, H. Lühr and C. Stolle (2018), On  
602 the variability of the semidiurnal solar and lunar tides of the equatorial electrojet during  
603 sudden stratospheric warmings, *Ann. Geophys.*, *36*, 1545–1562
- 604 Valladares, C. E., and J. L. Chau (2012), The Low-Latitude Ionosphere Sensor Network:  
605 Initial results, *Radio Sci.*, *47*(RS0L17), doi:10.1029/2011RS004978.
- 606 Venkatesh, K., P. R. Fagundes, D. S. V. V. D. Prasad, C. M. Denardini, A. J. de Abreu,  
607 R. de Jesus and M. Gende (2015), Day-to-day variability of equatorial electrojet and  
608 its role on the day-to-day characteristics of the equatorial ionization anomaly over  
609 the Indian and Brazilian sectors, *J. Geophys. Res. Space Physics*, *120*, 9117–9131, doi:  
610 10.1002/2015JA021307
- 611 Vineeth, C., T. K. Pant, and R. Sridharan (2009), Equatorial counter electrojets and po-  
612 lar stratospheric sudden warmings - A classical example of high latitude-low latitude  
613 coupling?, *Annales de Geophysique*, *27*, 3147–3153

- 614 Yizengaw, E., and M. B. Moldwin (2009), African Meridian B-field Education and Re-  
615 search (AMBER) Array, *Earth, Moon, and Planets*, doi:10.1007/s11038-008-9287-2.
- 616 Yizengaw, E., and K. M. Groves (2018), Longitudinal and Seasonal Variability of Equato-  
617 rial Ionospheric Irregularities and Electrodynamics, *Space Weather*, *16*(8), 946–968.
- 618 Yizengaw, E., M. B. Moldwin, E. Zesta, C. M. Biouele, B. Damtie, A. Mebrahtu, B. Ra-  
619 biu, C. E. Valladares, and R. Stoneback (2014), The longitudinal variability of equa-  
620 torial electrojet and vertical drift velocity in the African and American sectors, *Ann.*  
621 *Geophys.*, *32*, 231–238.
- 622 Yizengaw, E., M. B. Moldwin, A. Mebrahtu, B. Damtie, E. Zesta, C. E. Valladares, and  
623 P. H. Doherty (2011), Comparison of storm time equatorial ionospheric electrodynamics  
624 in the African and American sectors, *J. Atmos. Solar-Terr. Phys.*, *73*(1), 156–163.
- 625 Yizengaw, E., E. Zesta, M. B. Moldwin, B. Damtie, A. Mebrahtu, C. E. Valladares,  
626 and R. F. Pfaff (2012), Longitudinal differences of ionospheric vertical density dis-  
627 tribution and equatorial electrodynamics, *J. Geophys. Res. Space Phys.*, *A07312*,  
628 doi:10.1029/2011JA017454.
- 629 Zhou, Y.- L., H. Lüher, H.- W. Xu, and P. Alken (2018), Comprehensive anal-  
630 ysis of the counter equatorial electrojet: Average properties as deduced  
631 from CHAMP observations, *J. Geophys. Res. Space Phys.*, *123*, 5159–5181,  
632 <https://doi.org/10.1029/2018JA025526>.

### 633 Figure captions

634 Figure 1: Pairs of magnetometer locations (magenta filled circles) used to compute  
635 EEJ in the African and American sectors. The blue line represents the geomagnetic equa-  
636 tor. Black lines represent the crests of the equatorial ionization anomaly at  $\pm 15^\circ$ .

637 Figure 2: Examples of horizontal component of the geomagnetic field with derived  
638 EEJ changes and available C/NOFS vertical ion plasma drift ( $\mathbf{E} \times \mathbf{B}$  drift, plotted as black  
639 dots) for longitude sectors of (a)  $69^\circ\text{W}$  (23 November 2011), (b)  $56^\circ\text{W}$  (28 October 2012),  
640 (c)  $9^\circ\text{E}$  (23 January 2012), and (d)  $39^\circ\text{E}$  (19 November 2008) respectively.

641 Figure 3: Scatter plot of C/NOFS vertical  $\mathbf{E} \times \mathbf{B}$  drift against  $\Delta H$  over PUER (Amer-  
642 ican sector) and AAE (African sector) from 2008-2014. In (a) and (b), N represents the  
643 total number of data points

644 Figure 4: Local time observations of CEJ occurrences as observed from C/NOFS  
645 satellite and ground-based magnetometer data, separately during 2008-2010 and 2011-

646 2014 over (a) PUER (12.6°S, 69.2°W) and (b) ALTA (9.9°S, 56.1°W), within the Ameri-  
647 can sector.

648 Figure 5: Local time observations of CEJ occurrences as observed from C/NOFS  
649 satellite and ground-based magnetometer data, separately during 2008-2010 and 2011-  
650 2014 over (a) AAE (9.0°N, 38.8°E), and (b) ABJA (10.5°N, 7.6°E), within the African  
651 sector.

652 Figure 6: Percentage agreement for C/NOFS and  $\Delta H$  observations in identifying  
653 CEJ over (a) American sector, and (b) African sector, during 2008-2014

654 Figure 7: Seasonal occurrence of CEJ (expressed as a percentage) as observed by  
655 C/NOFS satellite (brown) and ground-based magnetometers (blue) over the American and  
656 African sectors during 2011-2014



Figure 1.

Author Manuscript

Pairs of magnetometer locations (magenta circles) used to compute the EEJ

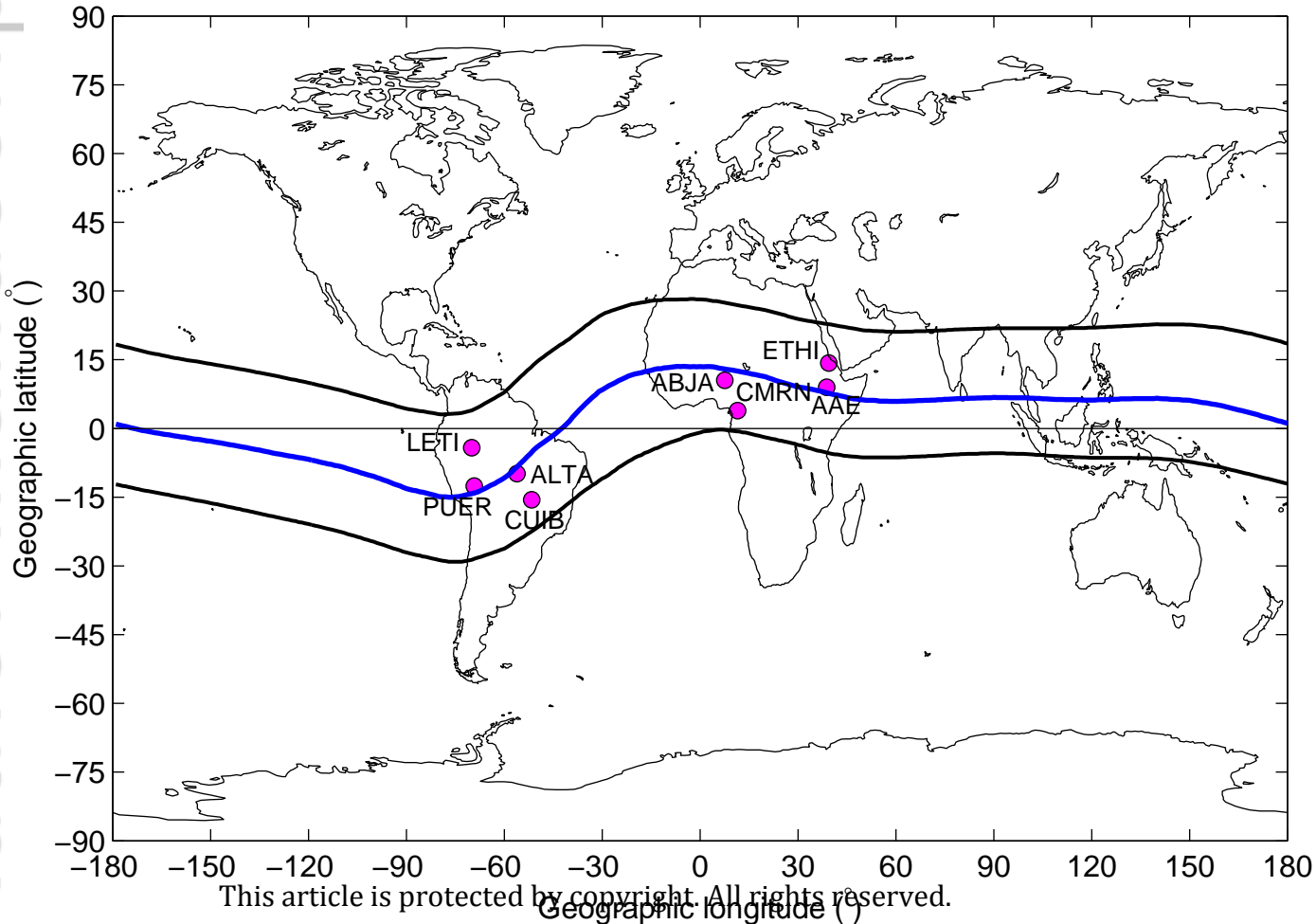
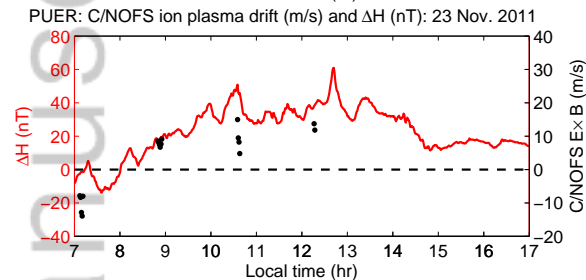
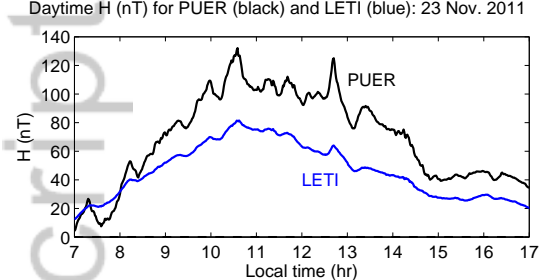
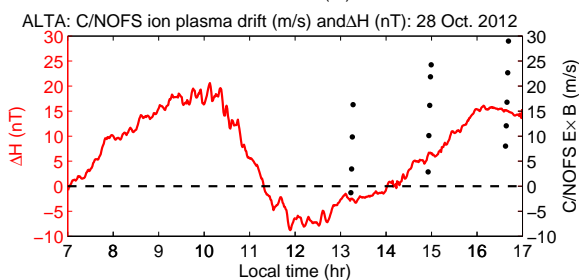
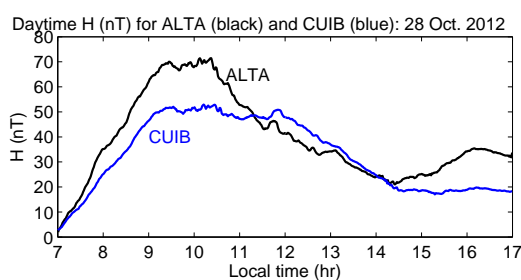


Figure 2.

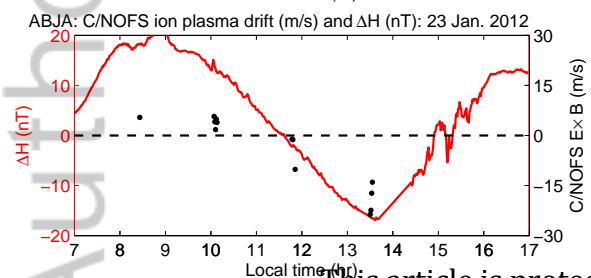
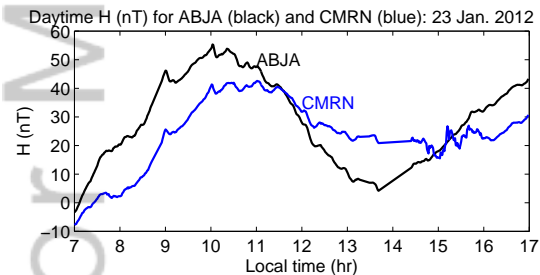
Author Manuscript



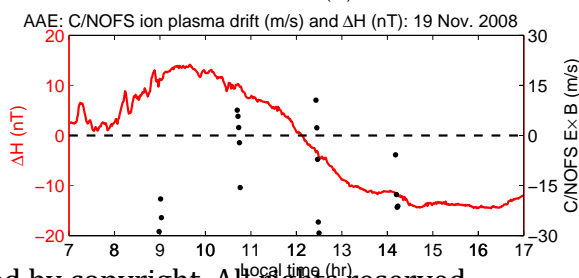
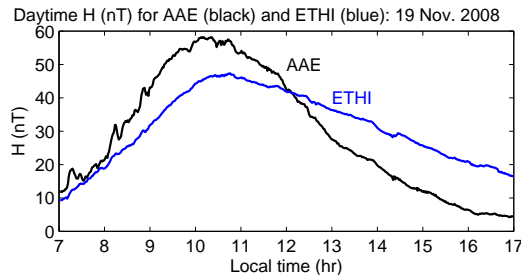
(a) PUER-LETI: 23 November 2011



(b) ALTA-CUIB: 28 October 2012



(c) ABJA-CMRN: 23 January 2012

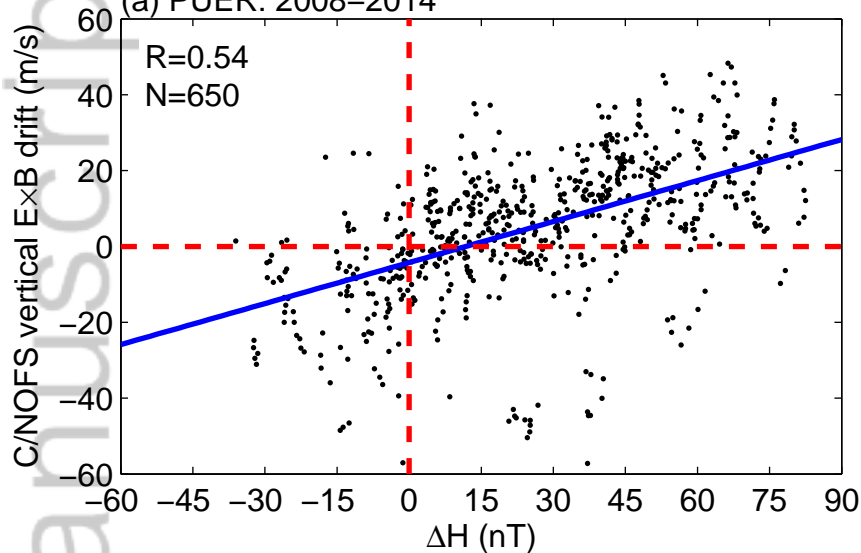


(d) AAE-ETHI: 19 November 2008

Figure 3.

Author Manuscript

(a) PUER: 2008–2014



(b) AAE: 2008–2014

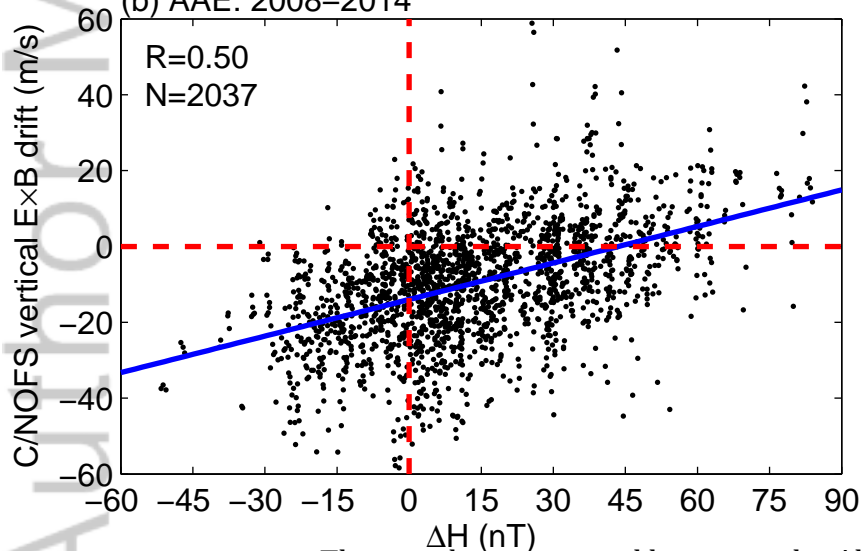
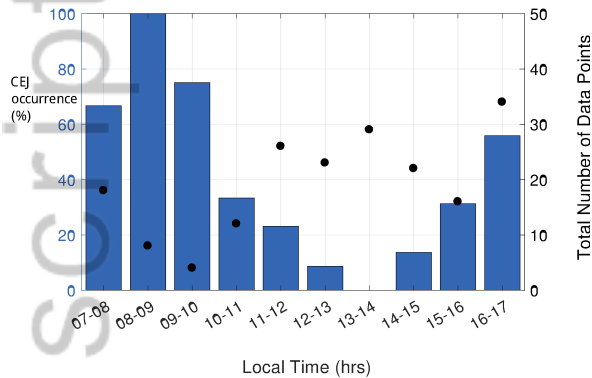


Figure 4.

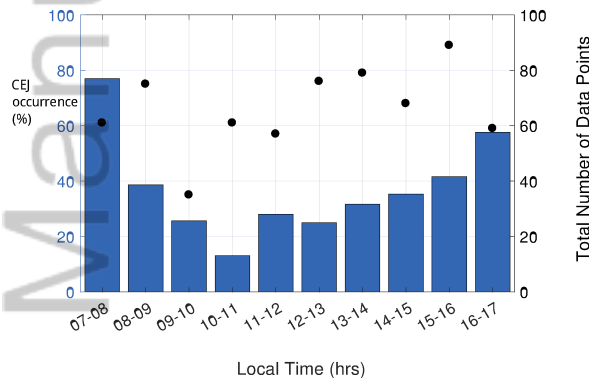
Author Manuscript



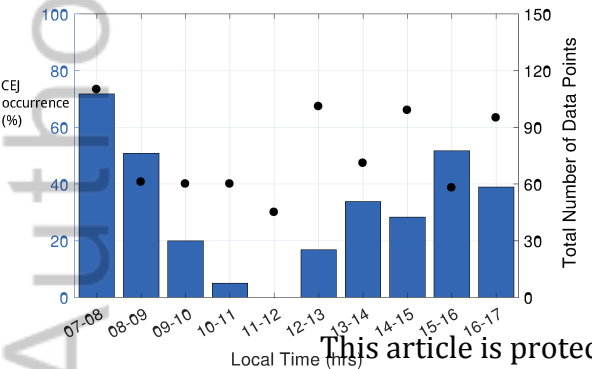
C/NOFS: 2008 - 2010



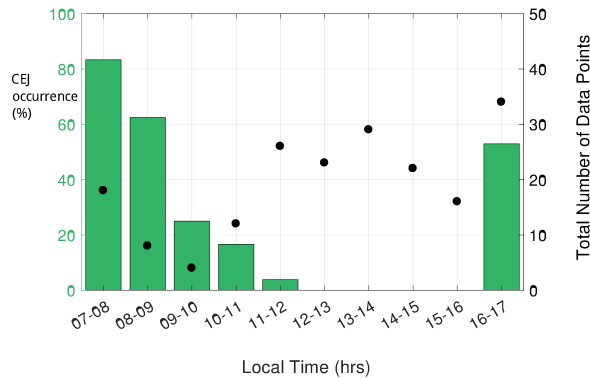
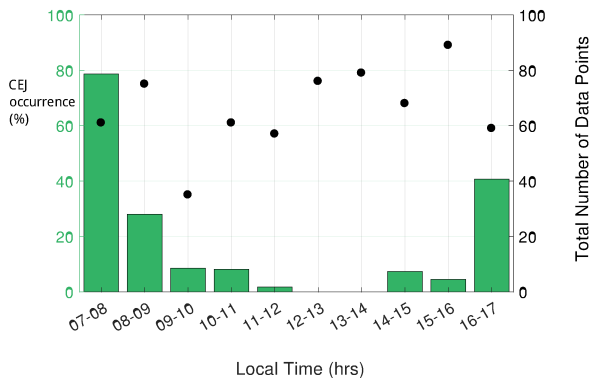
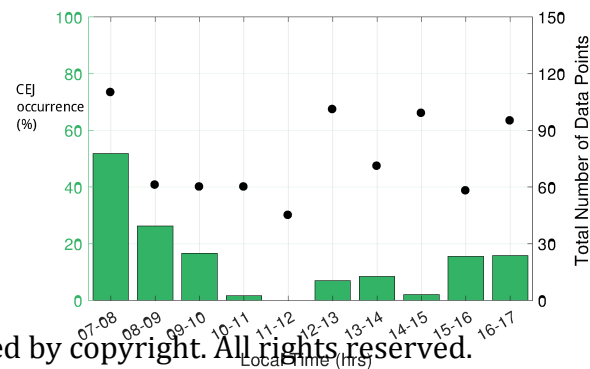
C/NOFS: 2011 - 2014



C/NOFS: 2011 - 2014



C/NOFS: 2011 - 2014

 $\Delta$ H: 2008 - 2010 $\Delta$ H: 2011 - 2014 $\Delta$ H: 2011 - 2014 $\Delta$ H: 2011 - 2014

(a) PUER (12.6°S, 69.2°W)

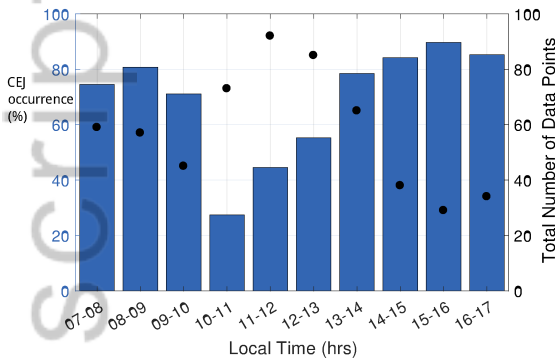
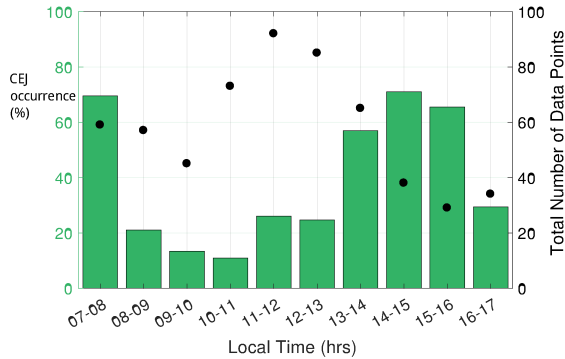
(b) ALTA (9.9°S, 56.1°W)

This article is protected by copyright. All rights reserved.

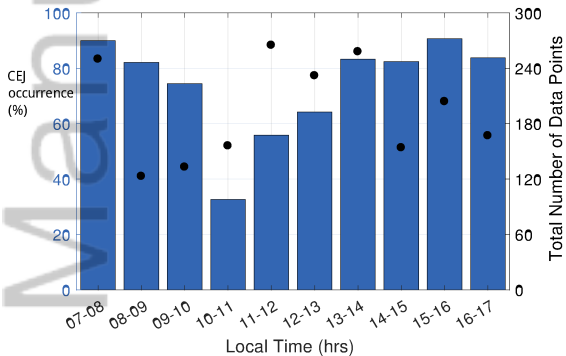
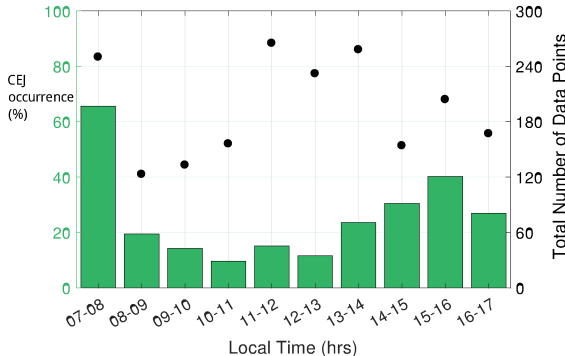
Figure 5.

Author Manuscript

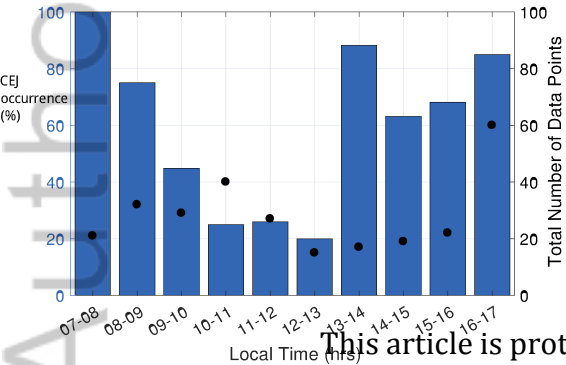
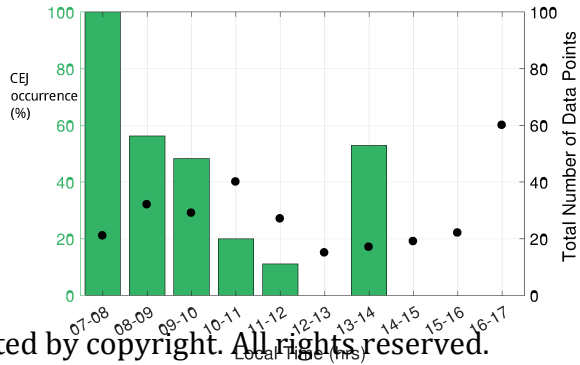
C/NOFS: 2008 - 2010

 $\Delta H$ : 2008 - 2010

C/NOFS: 2011 - 2014

 $\Delta H$ : 2011 - 2014(a) AAE ( $9.0^{\circ}\text{N}$ ,  $38.8^{\circ}\text{E}$ )

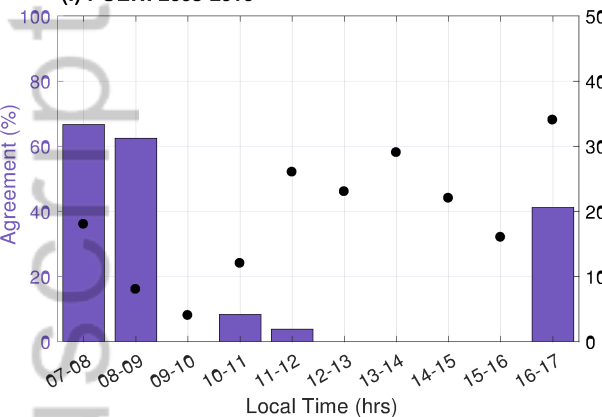
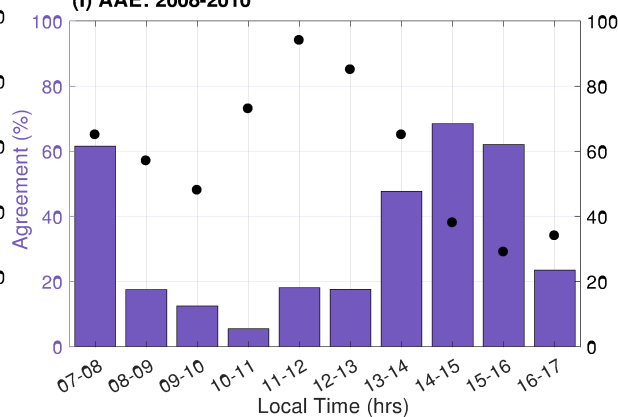
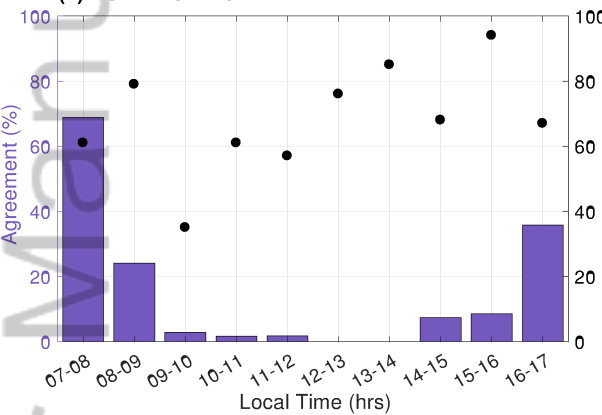
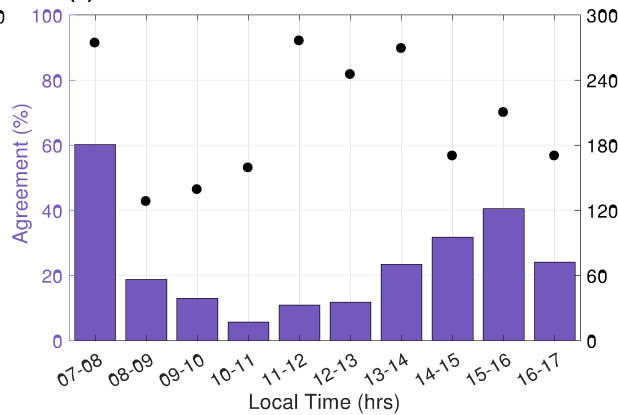
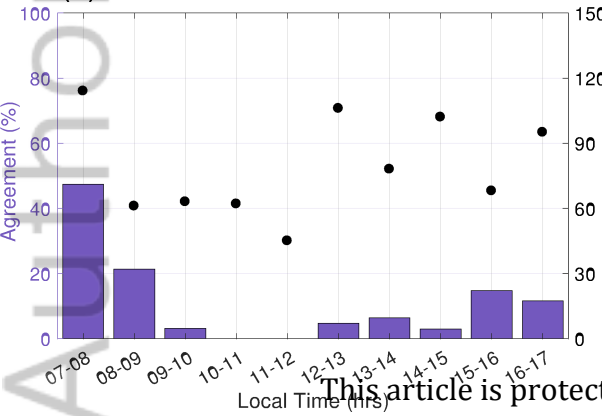
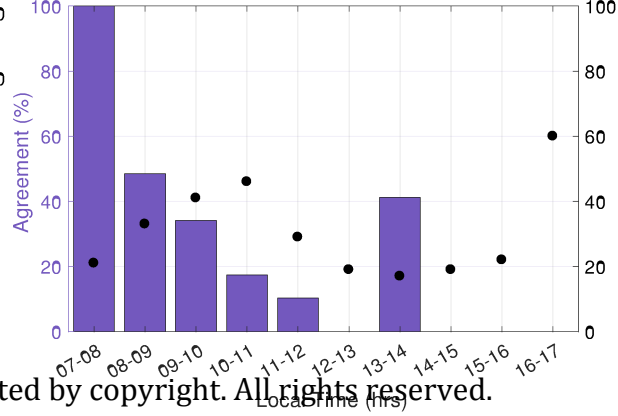
C/NOFS: 2011 - 2014

 $\Delta H$ : 2011 - 2014(b) ABJA ( $10.5^{\circ}\text{N}$ ,  $7.6^{\circ}\text{E}$ )

This article is protected by copyright. All rights reserved.

Figure 6.

Author Manuscript

**(I) PUER: 2008-2010****(I) AAE: 2008-2010****(II) PUER: 2011-2014****(II) AAE: 2011-2014****(III) ALTA: 2011-2014****(III) ABJA: 2011-2014**

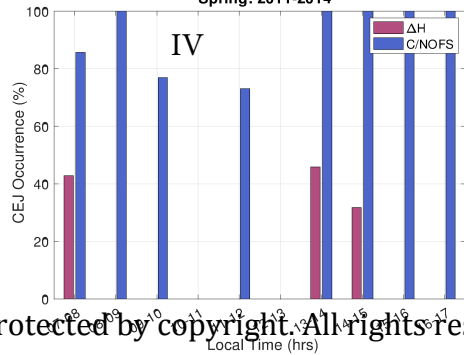
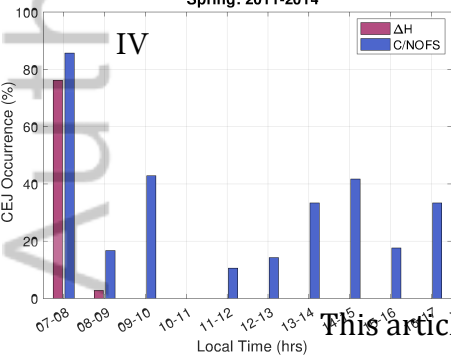
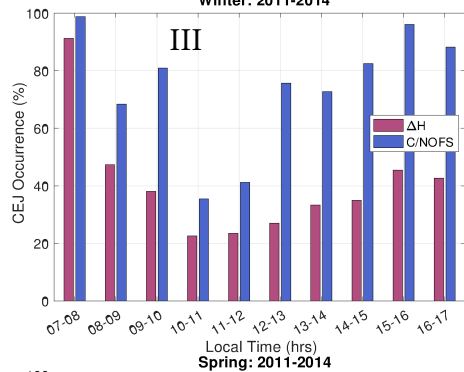
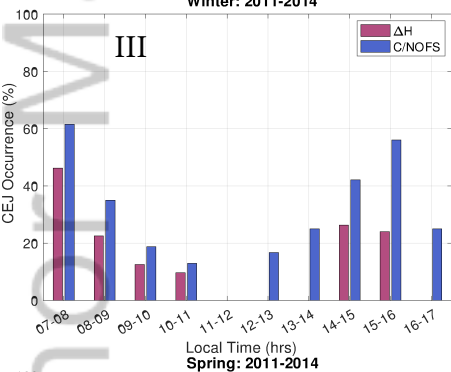
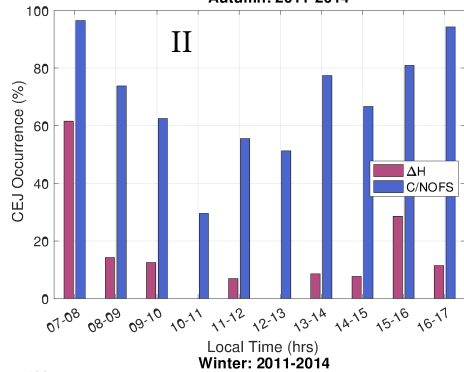
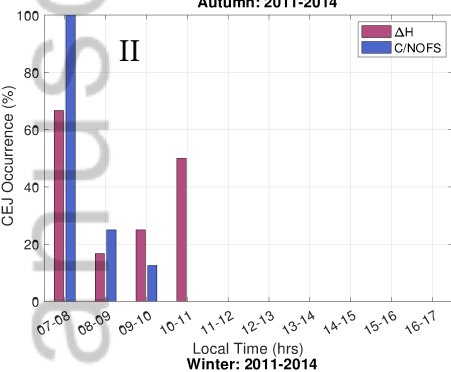
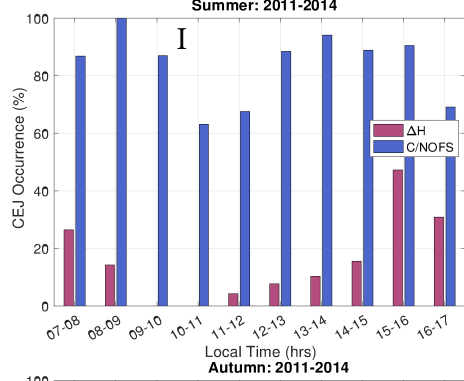
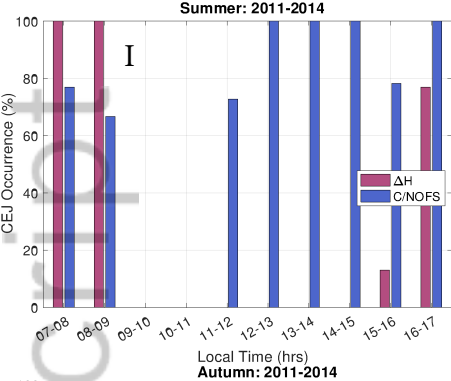
This article is protected by copyright. All rights reserved.

(a) American sector

(b) African sector

Figure 7.

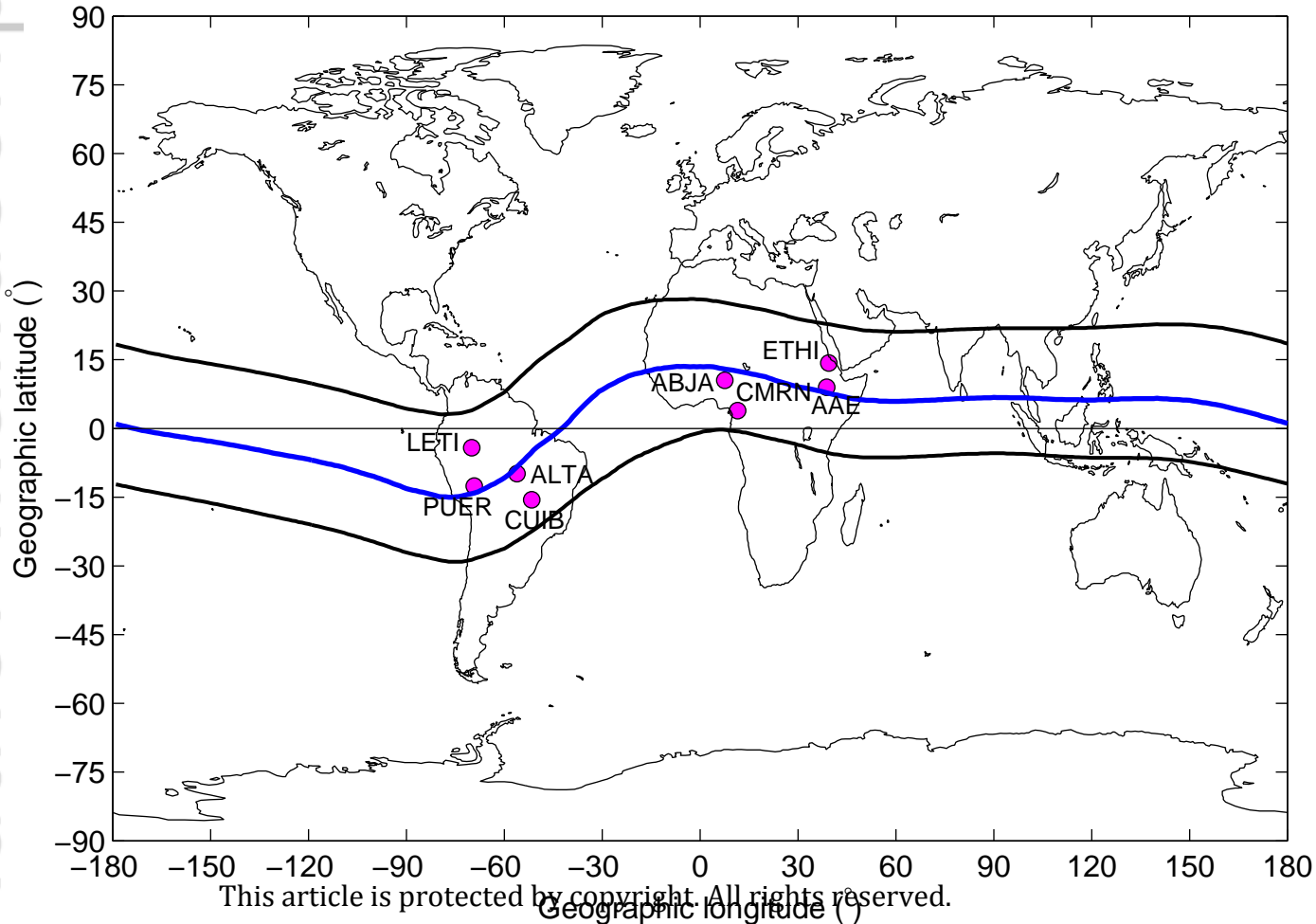
Author Manuscript



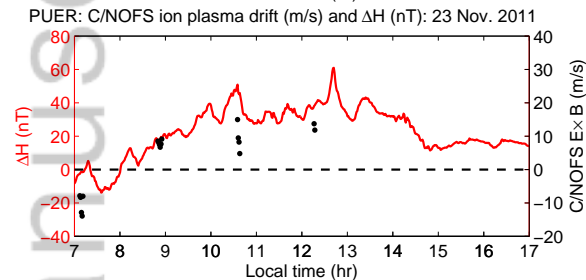
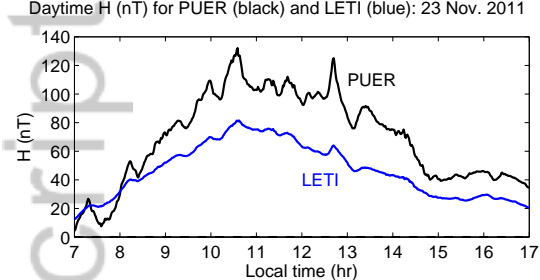
(a) Seasonal CEJ occurrence: PUER (12.6°S, 69.2°W)

(b) Seasonal CEJ occurrence: AAE (9.0°N, 38.8°E)

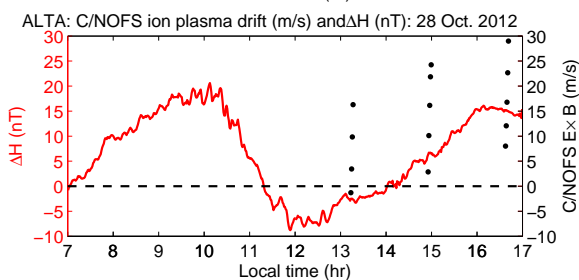
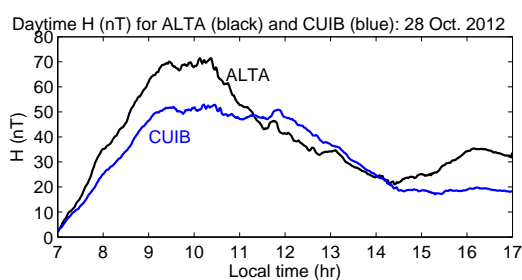
Pairs of magnetometer locations (magenta circles) used to compute the EEJ



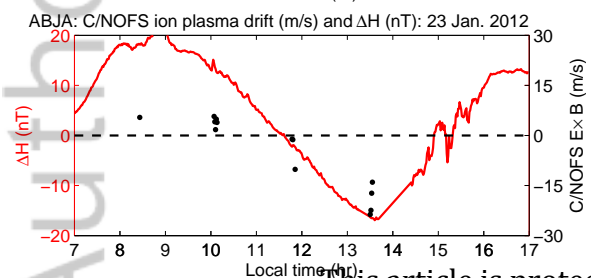
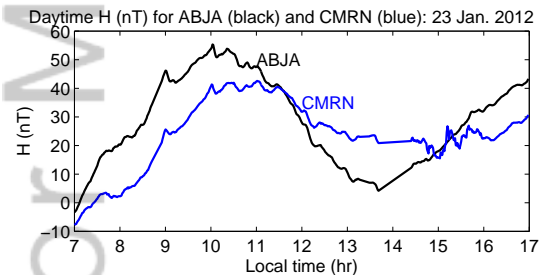




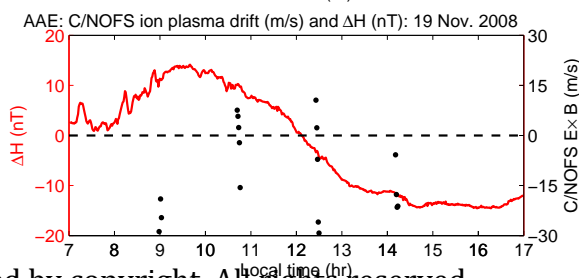
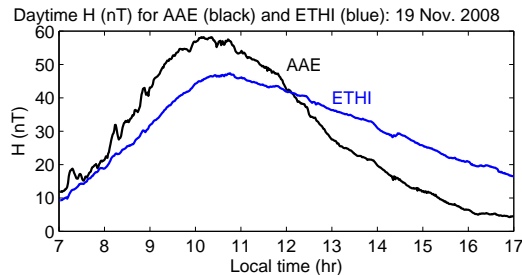
(a) PUER-LETI: 23 November 2011



(b) ALTA-CUIB: 28 October 2012

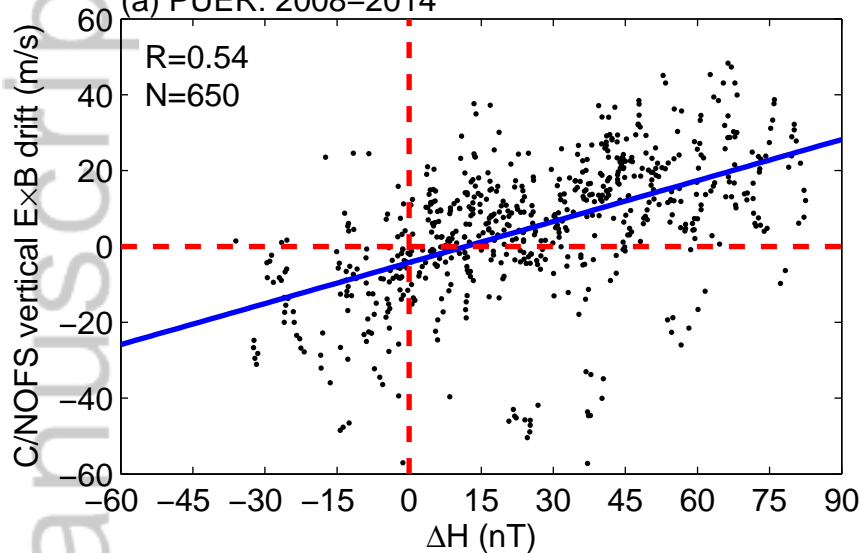


(c) ABJA-CMRN: 23 January 2012

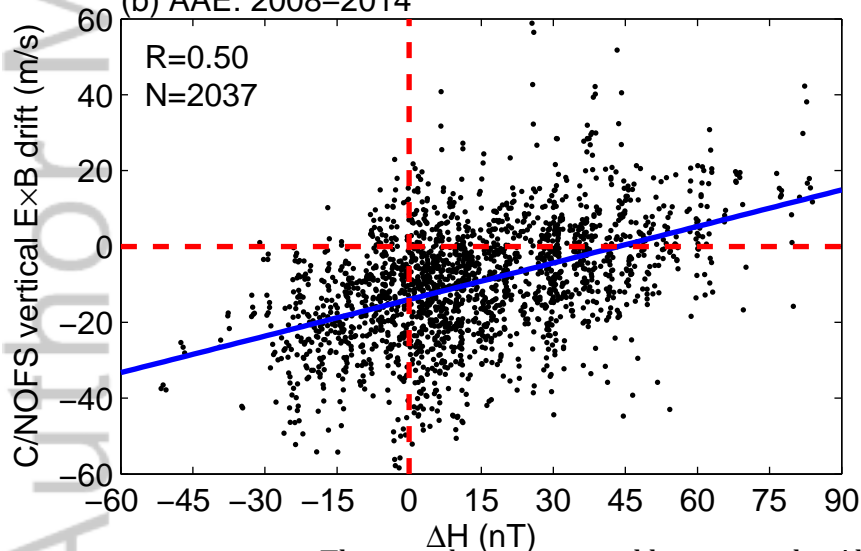


(d) AAE-ETHI: 19 November 2008

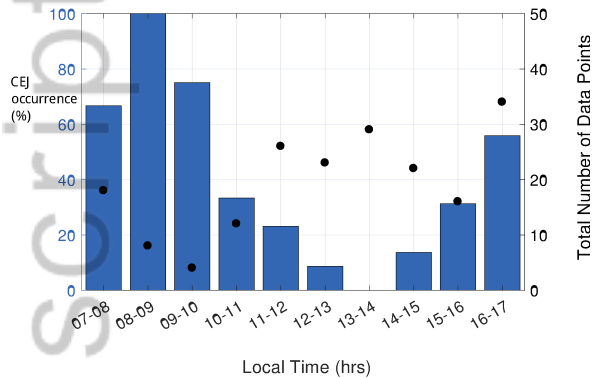
(a) PUER: 2008–2014



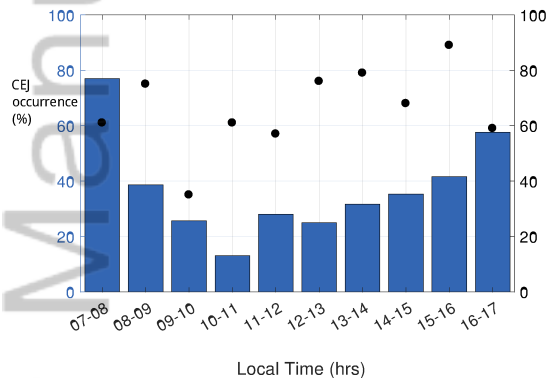
(b) AAE: 2008–2014



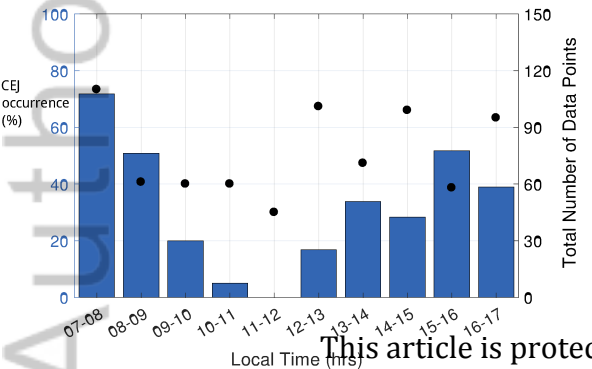
C/NOFS: 2008 - 2010



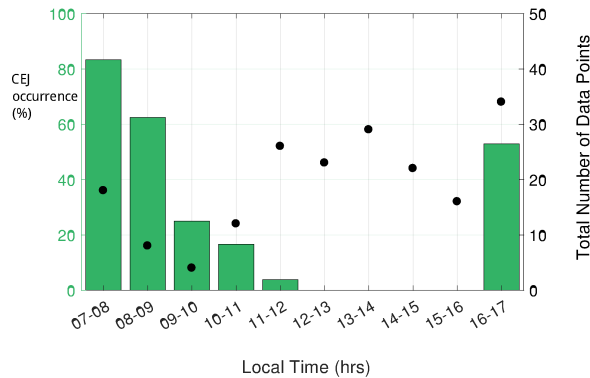
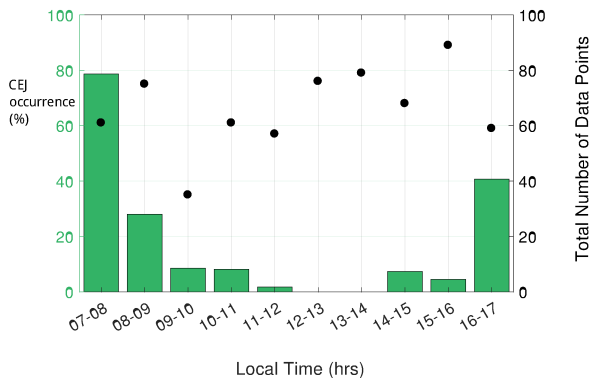
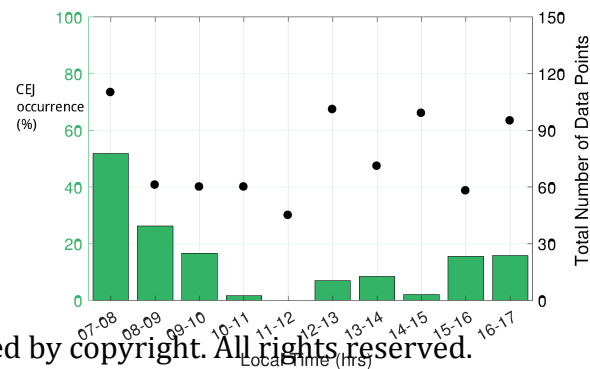
C/NOFS: 2011 - 2014



C/NOFS: 2011 - 2014



C/NOFS: 2011 - 2014

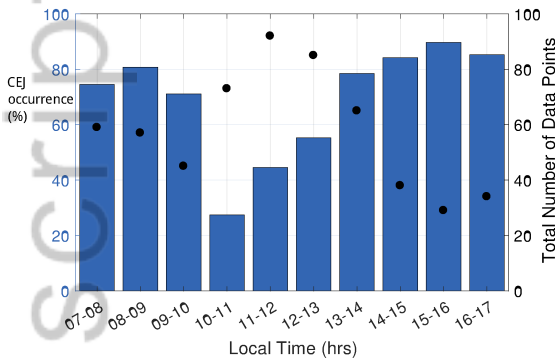
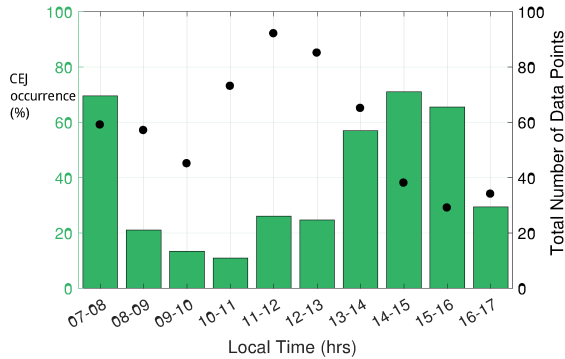
 $\Delta$ H: 2008 - 2010 $\Delta$ H: 2011 - 2014 $\Delta$ H: 2011 - 2014 $\Delta$ H: 2011 - 2014

(a) PUER (12.6°S, 69.2°W)

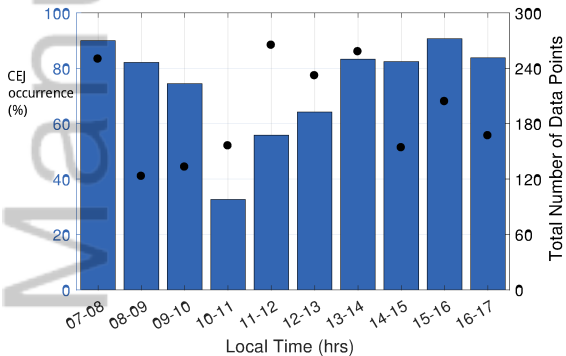
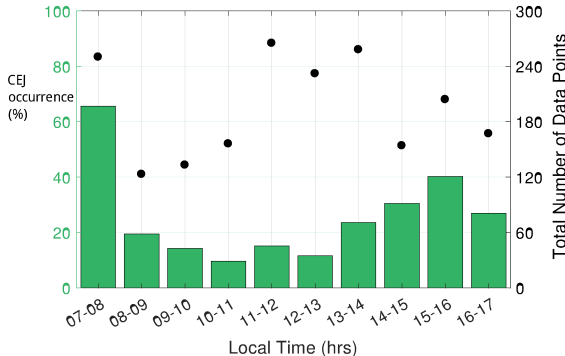
(b) ALTA (9.9°S, 56.1°W)

This article is protected by copyright. All rights reserved.

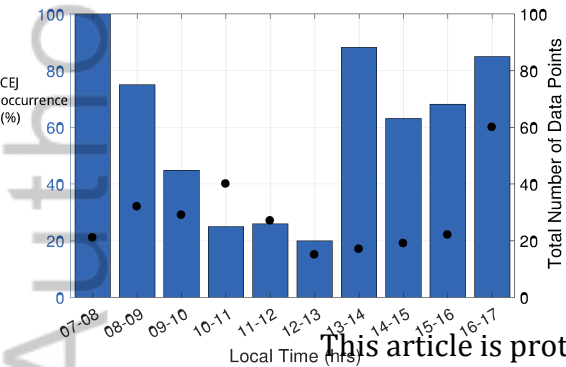
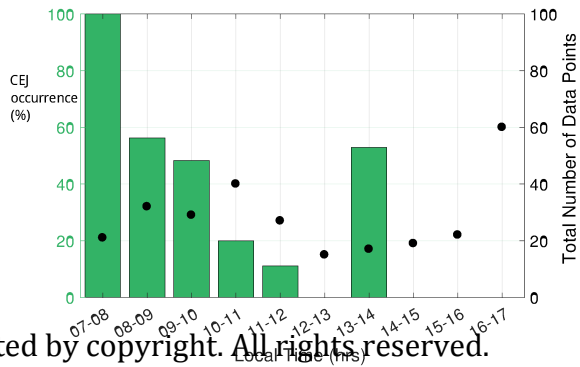
C/NOFS: 2008 - 2010

 $\Delta H$ : 2008 - 2010

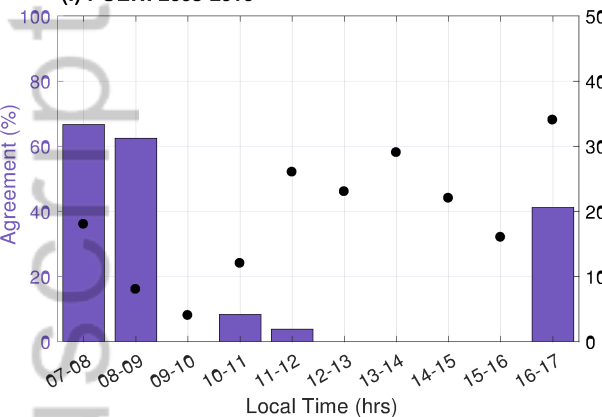
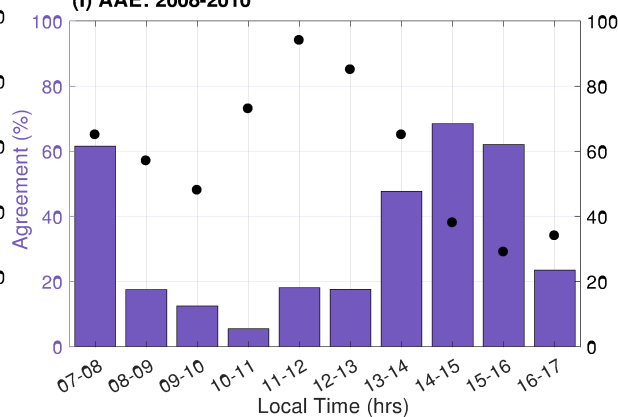
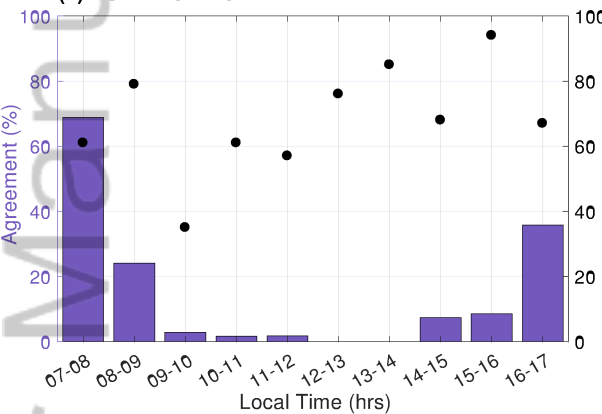
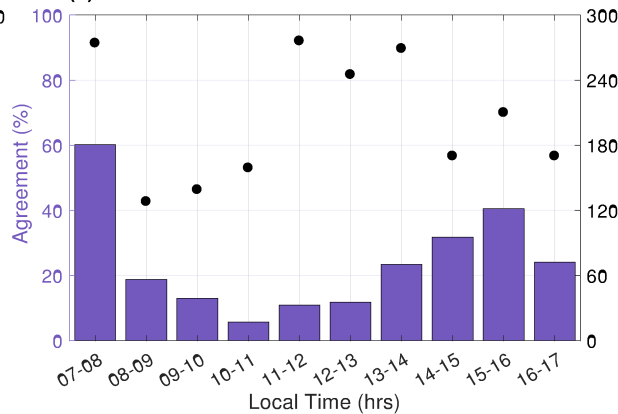
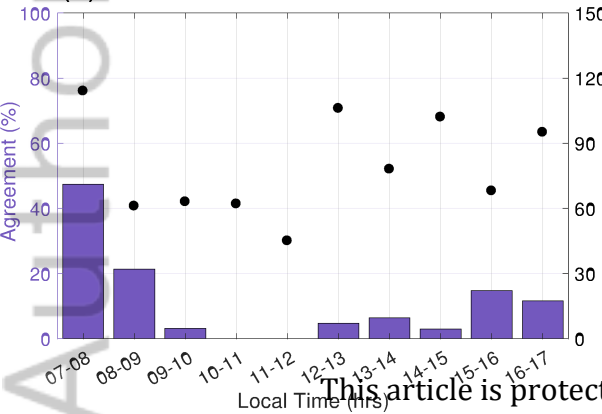
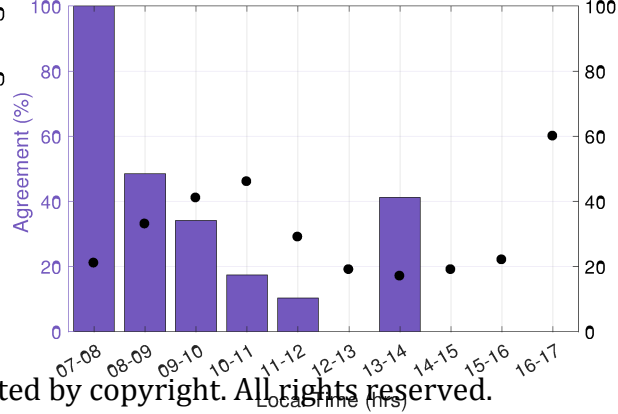
C/NOFS: 2011 - 2014

 $\Delta H$ : 2011 - 2014(a) AAE ( $9.0^{\circ}\text{N}$ ,  $38.8^{\circ}\text{E}$ )

C/NOFS: 2011 - 2014

 $\Delta H$ : 2011 - 2014(b) ABJA ( $10.5^{\circ}\text{N}$ ,  $7.6^{\circ}\text{E}$ )

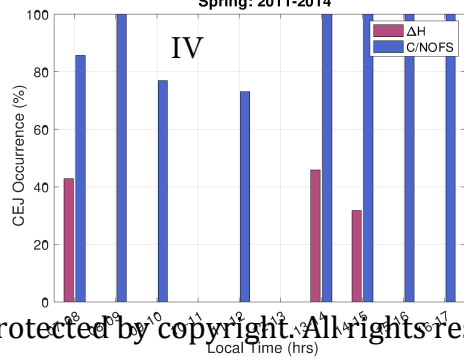
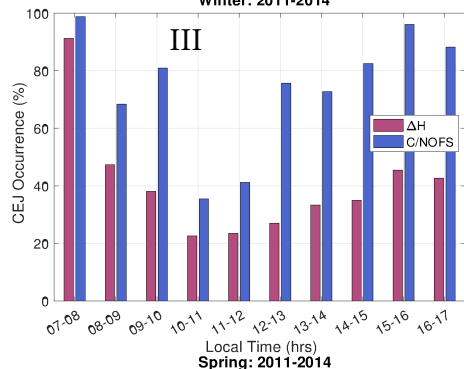
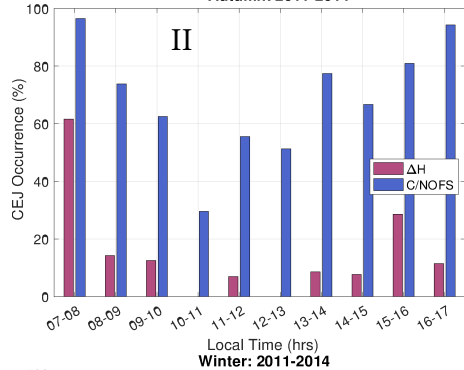
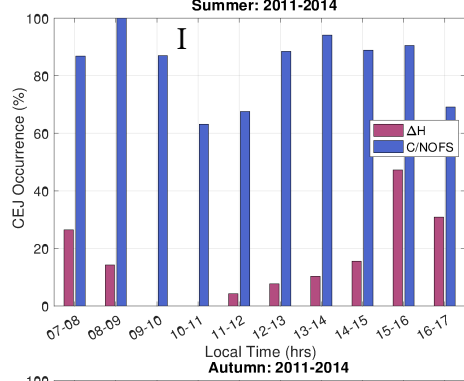
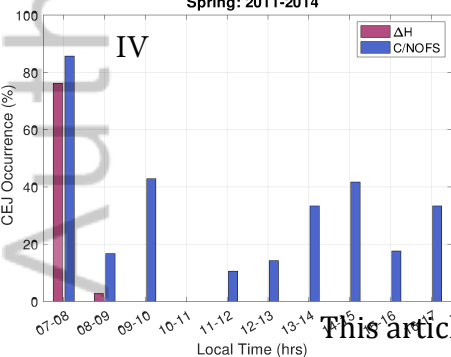
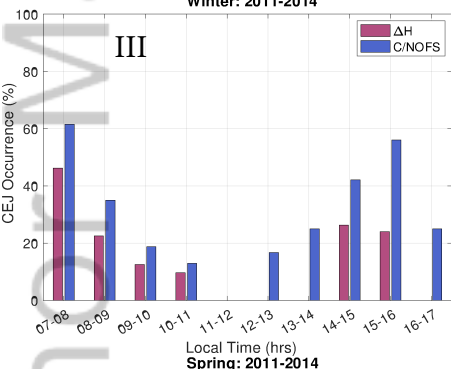
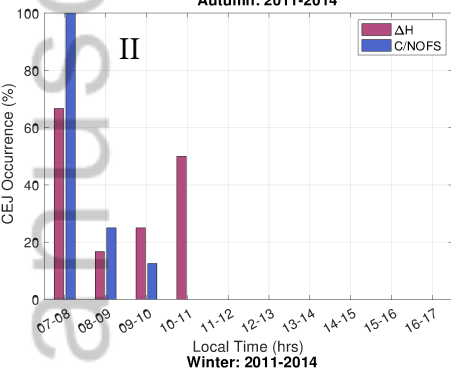
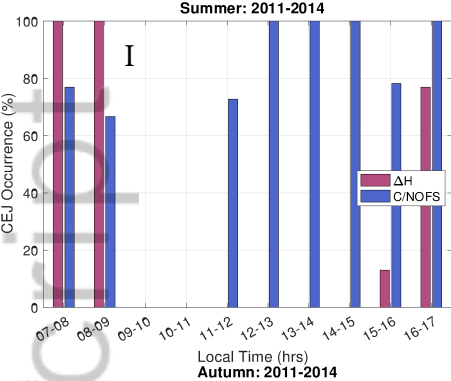
This article is protected by copyright. All rights reserved.

**(I) PUER: 2008-2010****(I) AAE: 2008-2010****(II) PUER: 2011-2014****(II) AAE: 2011-2014****(III) ALTA: 2011-2014****(III) ABJA: 2011-2014**

This article is protected by copyright. All rights reserved.

(a) American sector

(b) African sector



(a) Seasonal CEJ occurrence: PUER (12.6°S, 69.2°W)

(b) Seasonal CEJ occurrence: AAE (9.0°N, 38.8°E)